

AD-A194 875

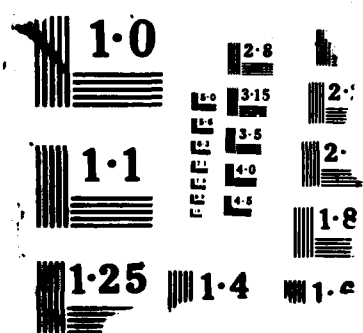
AN INVESTIGATION OF CONSTITUTIVE MODELS FOR PREDICTING  
VISCOPLASTIC RESPO (U) AIR FORCE INST OF TECH  
WRIGHT-PATTERSON AFB OH SCHOOL OF ENGI... D A SHAFFER  
JUN 88 AFIT/GAE/AA/87D-21 F/G 20/11

1/1

UNCLASSIFIED

NL

END



AD-A194 875



DTIC  
ELITE  
JUN 23 1988  
S H D

AN INVESTIGATION OF CONSTITUTIVE MODELS  
FOR PREDICTING VISCOPLASTIC RESPONSE  
DURING CYCLIC LOADING

THESIS

David A. Shaffer  
Captain, USAF

AFIT/GAE/AA/87D-21

DEPARTMENT OF THE AIR FORCE  
AIR UNIVERSITY

**AIR FORCE INSTITUTE OF TECHNOLOGY**

Wright-Patterson Air Force Base, Ohio

**DISTRIBUTION STATEMENT A**

Approved for public release;  
Distribution Unlimited

88 0 23 0 51

1

AN INVESTIGATION OF CONSTITUTIVE MODELS  
FOR PREDICTING VISCOPLASTIC RESPONSE  
DURING CYCLIC LOADING

THESIS

David A. Shaffer  
Captain, USAF

AFIT/ GAE/ AA/ 87D-21

RECEIVED  
JUN 23 1988  
RH

Approved for public release; distribution unlimited

AN INVESTIGATION OF CONSTITUTIVE MODELS  
FOR PREDICTING VISCOPLASTIC RESPONSE  
DURING CYCLIC LOADING

THESIS

Presented to the Faculty of the School of Engineering  
of the Air Force Institute of Technology  
Air University  
in Partial Fulfillment of the  
Requirements for the Degree of  
Master of Science

by

David A. Shaffer

Captain, USAF

Graduate Aerospace Engineering

June 1988

1

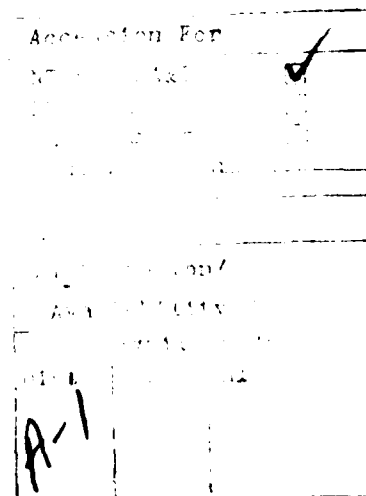


## Table of Contents

Acknowledgements .....	ii
List of Figures .....	iv
List of Tables .....	vi
List of Symbols .....	vii
Abstract .....	ix
I. Introduction .....	1
II. Literature Search .....	3
III. Description of Methods .....	5
Introduction .....	5
The Bodner-Partom Constitutive Law .....	5
Overstress Theory and Norton's Law for Secondary Creep .....	8
Time Step Selection .....	10
Additional Stability Criteria .....	11
IV. Results .....	13
Program Validation .....	13
Comparison of FINELS Output with Test Data .....	23
Computer Accuracy .....	24
Frequency Response of the Bodner-Partom Model .....	26
Frequency Response of the Overstress/Norton Model .....	38
Cyclic Creep (IN 100) .....	40
Simulated Stress Concentration .....	41
V. Conclusions .....	52
Summary of Work Done .....	52
Characteristics of the Bodner-Partom Model .....	52
Frequency Response .....	52
Creep Behavior .....	53
Kinematic Hardening .....	53
Time Step Size .....	53
Strain Softening .....	54
Numerical Instability .....	54
Simulated Stress Concentration .....	54
V. Recommendations .....	55
Creep in a Strain-Softening Material .....	55
Kinematic Hardening .....	55
Continued Investigation .....	55
Bibliography .....	56
Appendix A: Comparison of FINELS results with Stouffer's predictions .....	58
Appendix B: The Three-bar Linkage .....	61
Appendix C: Description of FEM code .....	65
Vita .....	85

## List of Figures

Figure	Page
1     IN 100 Time Convergence Study, $DT=0.1$ sec .....	14
2     IN 100 Time Convergence Study, $DT=0.05$ sec .....	15
3     IN 100 Time Convergence Study, $DT=0.01$ sec .....	16
4     IN 100 Time Convergence Study, $DT=0.005$ sec .....	17
5     IN 100 Time Convergence Study, $DT=0.001$ sec .....	18
6     IN 718 Time Convergence Study, $DT=0.1$ sec .....	20
7     IN 718 Time Convergence Study, $DT=0.05$ sec .....	21
8     IN 718 Time Convergence Study, $DT=0.01$ sec .....	22
9     Effect of Machine Accuracy upon Creep Predictions .....	25
10    IN 718 Prediction (Table I Material Properties, Initial Set) .....	27
11    Uniaxial Cyclic Strain Prediction (100 CPM) .....	28
12    Uniaxial Cyclic Strain Prediction (10 CPM) .....	29
13    Uniaxial Cyclic Strain Prediction (1 CPM) .....	30
14    Uniaxial Cyclic Strain Prediction (0.1 CPM) .....	31
15    Uniaxial Cyclic Strain Prediction (0.01 CPM) .....	32
16    Uniaxial Cyclic Strain Prediction (0.001 CPM) .....	33
17    Uniaxial Cyclic Stress Prediction (120 KSI, 6.7 CPM) .....	34
18    Uniaxial Cyclic Stress Prediction (150 KSI, 100 CPM) .....	36
19    Uniaxial Cyclic Stress Prediction (70 KSI, 0.001 CPM) .....	37
20    IN 100 Cyclic Stress Prediction (100 KSI, 0.001 CPM) .....	42
21    Simulated Stress Concentration (Three-Bar Linkage) .....	43
22    Stress vs. Time in a Viscoplastic Three-Bar Linkage .....	45
23    Stress Concentration Prediction (250 KPS, 100 CPM) .....	46



24	Stress Concentration Prediction (200 KPS, 1 CPM) .....	47
25	Stress Concentration Prediction (100 KPS, 0.001 CPM) .....	48
26	Plastic Strain vs. Frequency .....	50
A-1	Comparison of FINELS Output with Stouffer's Predictions (Tensile) .....	59
A-2	Comparison of FINELS Output with Stouffer's Predictions (Creep) .....	60
B-1	FINELS Three-Bar Linkage Viscoplastic Results .....	63
B-2	FINELS Three-Bar Linkage Viscoplastic and Creep Results .....	64

# List of Tables

Table	Page
I     Bodner-Partom Model Material Constants .....	8
II    Overstress/Norton's Law Material Constants .....	10
III   Matrix of Predicted Results, Bodner-Partom Model, Uniaxial Cy- clic Stress .....	26
IV    Matrix of Predicted Results, Overstress/Norton-Partom Model, Uniaxial Cyclic Stress .....	38
V     Matrix of Predicted Results, Bodner-Partom Model, Simulated Stress Concentration .....	41
VI    Matrix of Predicted Results, Overstress/Norton Model, Simulated Stress Concentration .....	49
VII   Three-Bar Linkage Conditions .....	62

## List of Symbols

$(\dot{\phantom{x}})$	Time rate of change of ( )
$A$	Bodner-Partom thermal recovery constant
$B$	Strain-displacement constant
$C$	Viscoplastic strain rate constant
$D_0$	Limit viscoplastic strain rate for the Bodner-Partom model
$D_2^P$	Second invariant of viscoplastic strain
$d(\phantom{x})$	Incremental change in ( )
$F$	Applied force
$J_2$	Second invariant of the deviatoric stress
$K$	Elastic stiffness
$L_n$	Length of element $n$
$m$	Strain hardening coefficient
$n$	Viscoplastic strain rate exponent
$Q$	Plastic force
$R$	Time step constant
$S_{ij}$	Deviatoric stress
$t$	Time
$W_p$	Plastic work
$X$	Yield criterion for the Overstress formulation
$Z$	Internal viscoplastic state variable
$Z_0$	Initial value of $Z$ for the Bodner-Partom model
$Z_1$	Saturation value of $Z$ for the Bodner-Partom model
$Z_i$	Lower limit of $Z$ for the Bodner-Partom model
$\dot{Z}_{rec}$	Rate of thermal recovery of plastic work for the Bodner-Partom model
$\beta$	Creep exponent for Norton's Law

$\epsilon$	Total strain
$\epsilon^E$	Elastic strain
$\epsilon^P$	Viscoplastic strain
$\epsilon^{VC}$	Viscoplastic creep strain
$\epsilon^Y$	Strain at yield point
$\epsilon^{inel}$	Inelastic strain
$\sigma$	Stress
$\sigma_0$	Normalizing stress for Norton's Law
$\sigma_Y$	Yield stress for the Overstress model
$\gamma$	Viscoplastic strain rate constant for the Overstress model
$\gamma_c$	Creep constant for Norton's Law

## I. Introduction

The Air Force's Engine Structural Integrity Program (ENSIP) (Ref 1) requires determination of damage tolerance for jet engine components in order to allow more economical rejection criteria to be adopted. To this end, means have been developed for predicting fatigue crack growth in jet engine components such as turbine disks made of nickel-based superalloys and operating at elevated temperatures. The presence of time-dependent plastic deformation greatly affects crack propagation rates, particularly at elevated temperatures and thus must be accounted for when modelling crack growth in turbine materials.

This plastic deformation in such materials takes two forms: That due to viscoplasticity and that due to creep. Viscoplasticity, as defined herein, occurs at high stresses and is characterized by large plastic deformation rates accompanied by changes in the material's internal state, typified by strain hardening or softening in which the material becomes more or less resistant to plastic flow. Creep, as defined herein, occurs at lower stresses and is characterized by small plastic strain rates while the material's internal state remains essentially unchanged. Viscoplastic deformation rate and creep rate are both functions of the magnitude and frequency of the applied strains and stresses. Finite element methods (FEM) can be used to predict crack growth in a component, but must incorporate a constitutive model that accounts for the viscoplasticity and creep which will occur at notches, crack tips, and other stress concentrations when the applied stress is sufficiently high.

A number of methods for modelling viscoplasticity and creep exist, some of which calculate viscoplasticity and creep via separate equations while others unify viscoplasticity and creep with a single equation which is valid for high and low inelastic strain rates. In reality the transition between creep and viscoplas-

ticity often occurs gradually over a range of stresses and strains, thereby making a unified model more consistent with actual material behavior. For this reason, a unified model was sought. One such model which the Air Force has investigated for crack growth prediction is the Bodner-Partom constitutive law (Ref 2).

→ The purpose of this thesis was to investigate the frequency response aspects of the Bodner-Partom constitutive law's behavior and to compare its results with those of other models and to cyclic and non-cyclic uniaxial tensile test data. ←

The investigation proceeded in several stages. First, two FEM codes were developed to model uniaxial viscoplasticity and creep, one using Bodner-Partom constitutive theory, the other a combination of Overstress Law and Norton's Law for Secondary Creep. The codes were then validated by comparison of their predictions with those of other, proven codes and with data taken from uniaxial tensile tests upon specimens subjected to cyclic stress and strain over a range of frequencies and amplitudes. The programs were then used to extrapolate uniaxial material behavior for conditions not covered by test data and to show material behavior at a stress concentration while under cyclic stress using a simple three-bar structural model.

## II. Literature Search

Available literature was reviewed in order to identify other ways by which viscoplasticity has been modelled and to find which models have been most useful for crack growth prediction.

The review turned up a number of viscoplasticity models, all of which have two elements in common: a means of relating inelastic strain rate to applied stress, and a means of accounting for strain hardening as a function of accumulated inelastic strain. Typical viscoplastic strain rate equations include:

Power Law (Refs 3,4,5):

$$\dot{\epsilon}^P = C \left( \frac{\sigma}{Z} \right)^n$$

Overstress (Refs 5,6):

$$\dot{\epsilon}^P = C \left( \frac{\sigma - X}{Z} \right)^n \quad (\sigma \geq X)$$

$$\dot{\epsilon}^P = 0 \quad (\sigma < X)$$

Exponential (Refs 2,4,7,8):

$$\dot{\epsilon}^P = C e^{-\left( \frac{Z}{\sigma} \right)^n}$$

Where  $\sigma$  is the applied stress,  $C$  and  $n$  are material constants,  $X$  determines the onset of plasticity for the Overstress model, and  $Z$  is a state parameter used to show hardening. Isotropic or non-directional hardening can be accounted for by making  $Z$  a function of accumulated plastic strain (Refs 2,3,5,7), while kinematic or directional hardening can be portrayed by adding to  $Z$ , terms whose value depends upon the direction of the applied stress (Refs 5,7,8). Ther-

mal recovery of hardening can also be shown, for which  $Z$  gradually evolves in the absence of applied stress. Alternately, in the Overstress model the parameter  $X$  can be used to portray strain-hardening and recovery by itself or in conjunction with  $Z$  (Refs 5,6).

Al' these equations can be used as unified constitutive laws (Refs 2-8). However, the exponential relationship has been found to best represent material behavior over a wide range of inelastic strain rates (Ref 7). For this reason, the Air Force has concentrated upon using the unified exponential constitutive law developed by Bodner and Partom (Ref 2). Mercer (Ref 9) and Hinnerichs (Ref 10) have used the Bodner-Partom constitutive law in FEM codes to account for viscoplasticity and creep while modelling crack growth in specimens subject to cyclic stress and sustained non-cyclic stress, respectively.



### III. Description of Methods

#### Introduction

In this section, it will be shown how inelastic strain rates are calculated and how hardening and recovery are portrayed by the Bodner-Partom model and by the combined Overstress/Norton's Law model. In addition, time step selection and other numerical stability criteria will be described.

#### The Bodner-Partom Constitutive Law

Bodner and Partom developed a constitutive relationship between applied stress and the rate of plastic deformation (Ref 2). The Bodner-Partom model can be used to predict viscoplasticity and creep and includes the effects of strain hardening/softening and thermal recovery.

The Bodner-Partom model relates plastic deformation rate to applied stress by using a state variable  $Z$  in the following manner:

$$\frac{1}{2} \dot{\epsilon}^P_{ij} \dot{\epsilon}^P_{ij} = D_2^P(J_2, Z) \quad (1)$$

where:

- $D_2^P$  is the second invariant of the plastic strain rate and is given by

$$D_2^P = D_0^2 \exp \left[ - \left( \frac{Z^2}{3J_2} \right)^n \frac{n+1}{n} \right] \quad (2)$$

- $J_2$  is the second invariant of the deviatoric stress.
- $D_0$  is the limiting value for the strain rate (for small strain rates, generally set at an arbitrarily high number such as  $1.0 \times 10^4$  sec).

- the parameter  $n$  determines the yield stress at a given strain rate.

In the uniaxial case,  $J_2 = \frac{1}{3}\sigma_{zz}^2$  and

$$\dot{\epsilon}_{zz}^P = \frac{2}{\sqrt{3}} \sqrt{D_2^P} \quad (3)$$

$$= \frac{2}{\sqrt{3}} D_0 \exp \left[ - \left( \frac{Z}{\sigma_{zz}} \right)^{2n} \left( \frac{n+1}{2n} \right) \right] \quad (4)$$

Isotropic strain hardening and softening is modelled by allowing the parameter  $Z$  to evolve as plastic strain accumulates:

$$Z = Z_1 - (Z_1 - Z_0) \exp(-m W_p) \quad (5)$$

where  $W_p$  is the plastic work and  $m$  is a material constant that determines the rate of change of  $Z$  and, by extension, the shape of the stress-strain curve for a given stress or strain rate.  $Z_0$  represents the initial value of  $Z$ , and  $Z_1$  represents the limiting value which  $Z$  will approach as plastic strain occurs. If the material exhibits strain hardening,  $Z_1$  is greater than  $Z_0$ . If the material exhibits strain softening,  $Z_1$  is less than  $Z_0$ .

In this investigation, the plastic work  $W_p$  is defined to include the net plastic strain energy plus an additional term to account for thermal recovery of hardening at elevated temperatures:

$$W_p = \int_0^t S_{ij} \dot{\epsilon}_{ij}^P dt + \int_0^t \frac{\dot{Z}_{rec}}{m(Z_1 - Z)} dt \quad (6)$$

$$= \int_0^t \sigma_{zz} \dot{\epsilon}_{zz}^P dt + \int_0^t \frac{\dot{Z}_{rec}}{m(Z_1 - Z)} dt \quad (\text{uniaxial case}) \quad (7)$$

where

$$\dot{Z}_{rec} = -AZ_1 \left( \frac{Z - Z_i}{Z_1} \right)^r \quad (8)$$

where  $Z_i$  represents a lower limit of  $Z$ , and  $A$  and  $r$  are additional material constants.

Viscoplastic stress and strain are calculated by Euler numerical integration over time. During each time step  $i$ , Equations (3) through (8) are performed for each element:

$$Z^i = Z_1 - (Z_1 - Z_0) \exp[-m W_p^{i-1}] \quad (9)$$

$$[D_2^P]^i = D_0^2 \exp \left[ - \left( \frac{Z^i}{\sigma_{zz}^i} \right)^{2n} \left( \frac{n+1}{n} \right) \right] \quad (10)$$

$$[\dot{\epsilon}_{zz}^P]^i = \frac{2}{\sqrt{3}} \sqrt{[D_2^P]^i} \quad (11)$$

$$[d\epsilon_{zz}^P]^i = [\dot{\epsilon}_{zz}^P]^i dt^i \quad (12)$$

$$W_p^i = W_p^{i-1} + \sigma_{zz}^i [d\epsilon_{zz}^P]^i + [\dot{Z}_{rec}]^i \left[ \frac{dt^i}{m(Z_1 - Z^i)} \right] \quad (13)$$

The material constants are determined via test data for the required temperature. Stouffer (Ref 11) shows how to obtain material parameters  $Z_1$ ,  $Z_0$ ,  $Z_i$ ,  $A$ ,  $m$ ,  $n$ , and  $r$  from uniaxial tensile stress-strain tests and creep tests at different stress and strain levels. The specific material parameter values used in this investigation are shown in Table I for turbine materials IN 100 and Inconel 718.

Note that for this investigation only isotropic or non-directional hardening has been incorporated into the Bodner-Partom model. Kinematic or directional hardening requires the calculation of several additional material parameters and their evolution rates during each time step and so, for simplicity, was not modelled. If required, the methods described by Lindholm, et al (Ref 7) and by Beaman (Ref 8) could be incorporated into the model.

Table I. Bodner-Partom Material Constants			
Parameter	IN 100 (Ref 11)	Inconel 718 (initial - Refs 8, 11)	Inconel 718 (revised)
$Z_0$	915.0 KSI	235.3 KSI	1,407.5 KSI
$Z_1$	1,015.0 KSI	260.3 KSI	1,245.0 KSI
$D_0$	$10^4/\text{sec}$	$10^6/\text{sec}$	$10^4/\text{sec}$
$n$	0.7	3.0	0.512
$m$	2.57/KSI	2.875/KSI	1.0/KSI
$Z_i$	600.0 KSI	104.1 KSI	500.0 KSI
$A$	$0.0019/\text{sec}$	$0.0015/\text{sec}$	$0.0015/\text{sec}$
$r$	2.66	7.0	7.0

### Overstress Theory and Norton's Law for Secondary Creep

The overstress formulation used was that developed by Perzyna (Ref 12). In this case, viscoplastic strain rate is determined as a function of applied stress by assuming the following relationship:

$$\dot{\epsilon}^P_{ij} = \gamma \left[ \frac{\sqrt{3J_2}}{\sigma_Y} - 1 \right]^n \left( \frac{3}{2} \frac{S_{ij}}{\sqrt{3J_2}} \right) \quad (\sqrt{3J_2} \geq \sigma_Y) \quad (14)$$

$$= 0 \quad (\sqrt{3J_2} < \sigma_Y)$$

where  $\gamma$  and  $n$  are material constants determined from uniaxial tensile stress-strain test data,  $S_{ij}$  are the components of the deviatoric stress tensor, and  $\sigma_Y$  is the material's yield stress. Strain hardening and softening is simulated by making the yield stress a function of plastic strain. In the uniaxial case,  $S_{ij} = \frac{2}{3}\sigma_{xx}$  and Equation (14) becomes

$$\dot{\epsilon}^P_{xx} = \gamma \left[ \frac{\sigma_{xx}}{\sigma_Y} - 1 \right]^n \quad (\sigma_{xx} \geq \sigma_Y) \quad (15)$$

$$= 0 \quad (\sigma_{xx} < \sigma_Y)$$

Since the overstress law only calculates viscoplasticity when the applied stress exceeds the yield stress, another law is needed to account for creep at lower stress levels. Norton's Law for Secondary Creep is a special case of the Power Law in which a constant internal state is assumed, making creep strain rate dependent only upon applied stress with no strain hardening or softening. Creep strain rate is predicted to be

$$\dot{\epsilon}^{VC}_{ij} = \gamma_c \left( \frac{\sqrt{3} J_2}{\sigma_0} \right)^\beta \quad (16)$$

where  $\gamma_c$  and  $\beta$  are material constants determined from creep tests conducted at two different stress levels, and  $\sigma_0$  is a normalizing stress generally given an arbitrary value such as 100 KSI. In the uniaxial case, Equation (16) becomes

$$\dot{\epsilon}^{VC}_{xx} = \gamma_c \left( \frac{\sigma_{xx}}{\sigma_0} \right)^\beta \quad (17)$$

The numerical Euler time integration is less involved than that required for the Bodner-Partom model, consisting of the following steps performed during each time step:

$$[\dot{\epsilon}^P_{xx}]^i = \gamma \left[ \frac{\sigma_{xx}^i}{\sigma_Y} - 1 \right] \quad (18)$$

$$[\dot{\epsilon}^{VC}_{xx}]^i = \gamma_c \left( \frac{\sigma_{xx}^i}{\sigma_0} \right)^\beta \quad (19)$$

$$[d\epsilon^{inel}]^i = \left( [\dot{\epsilon}^P_{xx}]^i + [\dot{\epsilon}^{VC}_{xx}]^i \right) dt^i \quad (20)$$

The material parameters used in this investigation for the Overstress/Norton's Law model were calculated from cyclic test data and are shown in Table II.

Table II. Overstress/Norton's Law Model Material Constants	
Material: Inconel 718 @1200 F	
Parameter	Value
$\gamma$	0.0107/sec
$n$	1.0
$\gamma_c$	$1.520 \times 10^{-26}$ /sec
$\sigma_0$	1.0 PSI
$\beta$	4.022

### Time Step Selection

For stable, accurate results, the time increment  $dt$  must not exceed the maximum allowable value for the model used. Cormeau (Ref 13) shows how to determine maximum time step sizes for Euler time integration schemes by using matrix algebra to find eigenvalues for the simultaneous differential equations involved. In two or more dimensions the calculations are somewhat cumbersome, however in the uniaxial case the procedure simplifies to

$$dt_{max} = \frac{2}{\lambda} \quad (21)$$

where

$$\lambda = EH \quad (22)$$

and

$$H = \frac{\partial \dot{\epsilon}^P}{\partial \sigma} \quad (23)$$

For the uniaxial Overstress and Norton models,

$$dt_{max} = \frac{2\sigma\gamma}{\gamma E} \quad (\text{Overstress, } n = 1) \quad (24)$$

$$dt_{max} = \frac{2}{\gamma_c E \beta (\sigma_{ss}^{\beta-1})} \quad (\text{Norton}) \quad (25)$$

Maximum time steps for the Bodner-Partom model can also be calculated for a given stress level:

$$dt_{\max} = R \sigma_{ss} \left( \frac{\sigma_{ss}}{Z} \right)^{2n} \exp \left( \frac{Z}{\sigma_{ss}} \right)^{2n} \quad (26)$$

where

$$R = \frac{\sqrt{3}}{ED_0(n+1)} \exp \left( \frac{n+1}{2n} \right)$$

In general, the maximum allowable time step during viscoplastic deformation will be several orders of magnitude smaller than the maximum allowable time step during creep. For stress-strain predictions in which stresses or strain rates vary between high and low values it is therefore often desirable to vary the time step size during program execution in order to reduce the total number of iterations required. Hinnerichs (Ref 10) describes a method for varying the time step size based on the changes in stress and strain which occur during a given time step. For simplicity, FINELS does not vary the time step, although such a method could be incorporated if necessary.

#### Additional Stability Criteria

For integration of a model which contains an evolving internal state variable, proper time step selection is necessary but not sufficient for ensuring numerical stability. Ponter (Ref 14) shows that for stability,

$$d\sigma d\dot{\epsilon}^P - dZ d\dot{Z} \geq 0 \quad (27)$$

during each time step, where  $d\sigma$ ,  $d\dot{\epsilon}^P$ ,  $dZ$ , and  $d\dot{Z}$  represent increments in stress, inelastic strain rate, internal state variable, and evolution rate of the internal state variable, respectively.

In general, viscoplasticity models will be unconditionally stable when strain hardening is modelled (Refs 7,14). Such models will only become conditionally stable when recovery rates are large. Strain softening models, on the other hand, are only conditionally stable when the increments in stress and strain rate are large compared with those of the internal variable and its evolution rate (Refs 7,14). This limits the ability of viscoplasticity models to predict the behavior of strain softening materials, especially at high applied stresses and low frequencies where the model is most likely to become unstable. This did in fact occur and is documented in Section IV.



## IV. Results

### Program Validation

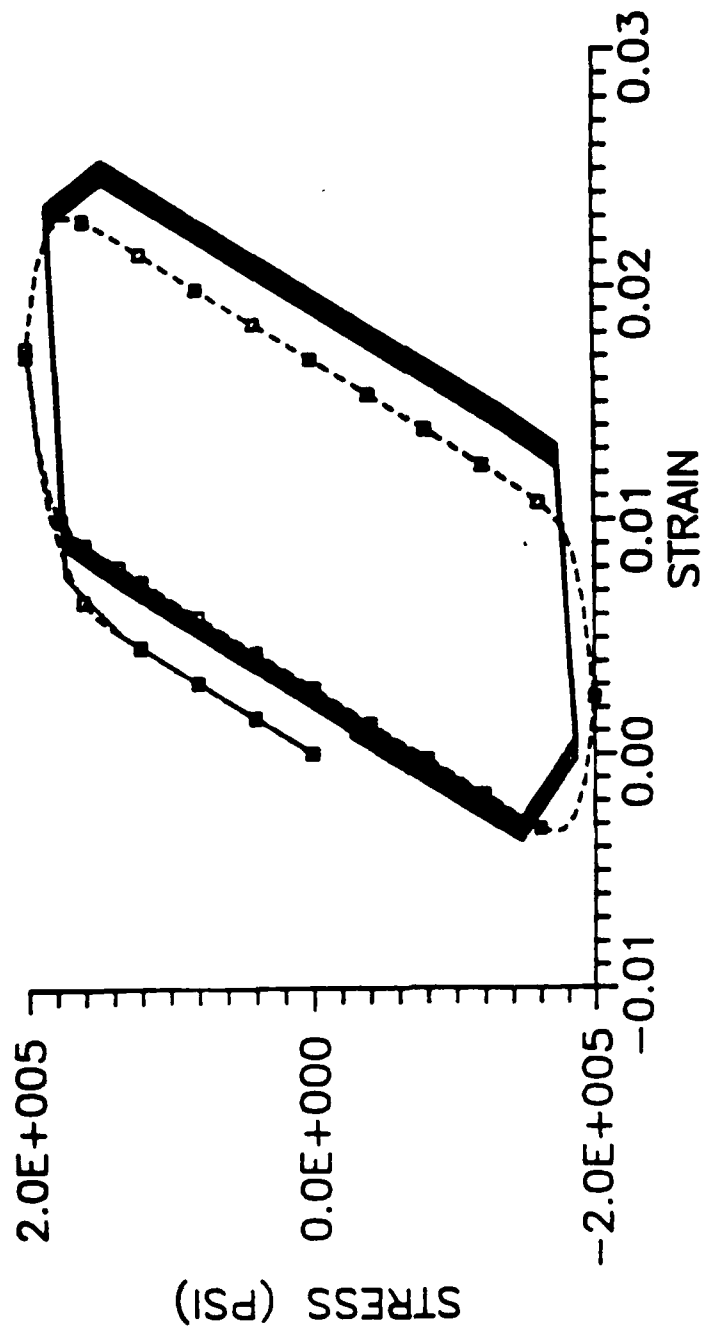
The program used for this investigation was FINELS (See Appendix C), a FORTRAN code developed to model viscoplasticity and creep in systems of uniaxial bars using finite element methods.

A time step convergence study was undertaken for FINELS in order to verify the program's accuracy and to validate the maximum time step size requirement. The test problem described by Mercer (Ref 9) was chosen, in which the program predicts the behavior of a uniaxial bar made of IN 100 subjected to cyclic stress of  $\pm 200$  KSI peak values applied at a frequency of 10 cpm. The problem was run using time steps of 0.1, 0.05, 0.01, 0.005, and 0.001 seconds. For a time step  $dt$  of 0.1 seconds, pronounced ratcheting was evident as the stress-strain loop shifted in the direction of decreasing strain with each applied stress cycle. For  $dt = 0.05$  seconds, the ratcheting was no longer evident although the stress-strain curve does not match Mercer's. For  $dt = 0.01$  seconds, the curves match more closely and for  $dt = 0.005$  seconds and  $dt = 0.001$  seconds, the FINELS curve is almost identical to Mercer's (See Figures 1 through 5).

The ratcheting phenomenon appears to be related to the numerical stability of the model. Using the Bodner-Partom material constants shown in Table I for IN 100, for  $\pm 200$  KSI peak stress the maximum allowable time step given by Equation 26 is

$$dt_{max} = 0.009 \text{ seconds}$$

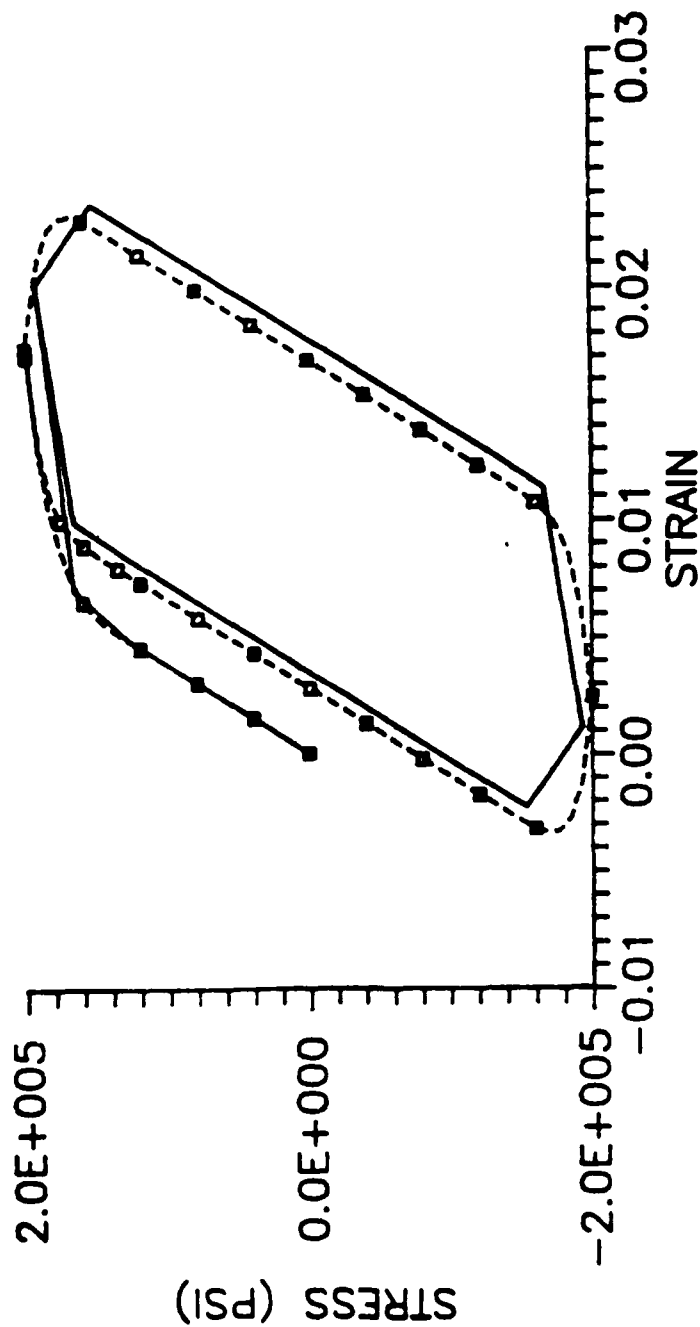
The inaccuracies and ratcheting shown for  $dt = 0.01$  seconds, 0.05 seconds, and 0.1 seconds respectively indicate that the model is not stable for these time step sizes. The maximum time step size therefore appears to be valid since



Frequency = 10 cpm  
 Peak stress = +/- 200 KSI

Dashed lines and symbols show  
 validated model results.  
 Solid lines show FINELS program  
 predictions.

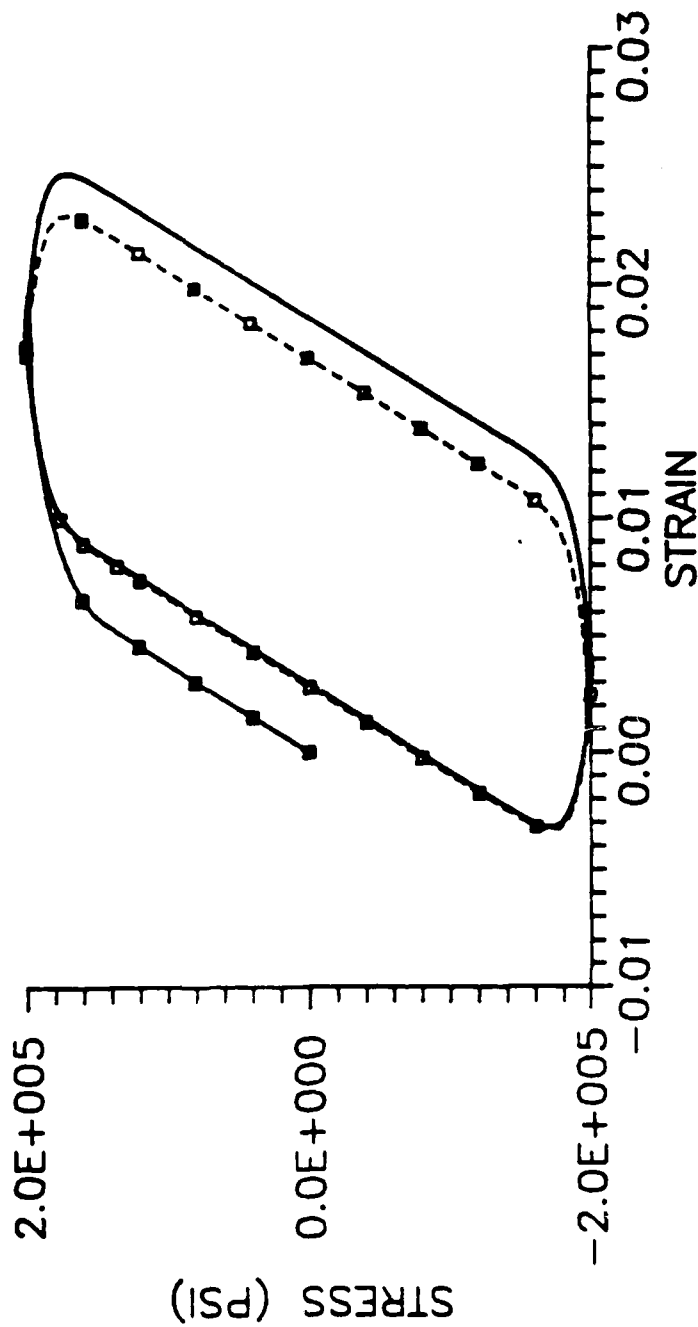
Figure 1. IN 100 Time Convergence Study, DT = 0.1 sec.



Frequency = 10 cpm  
 Peak stress = +/- 200 KSI

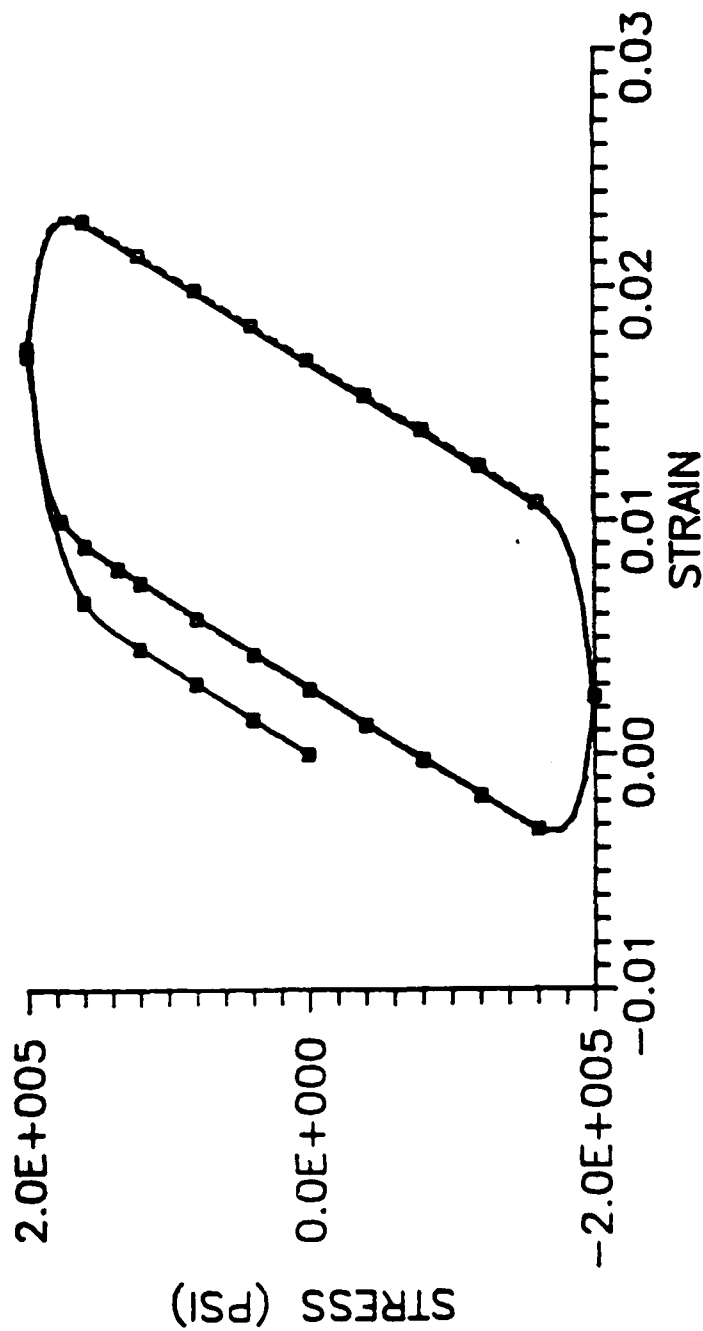
Dashed lines and symbols show  
 validated model results.  
 Solid lines show FINELS program  
 predictions.

Figure 2. IN 100 Time Convergence Study,  $DT = 0.05$  sec.



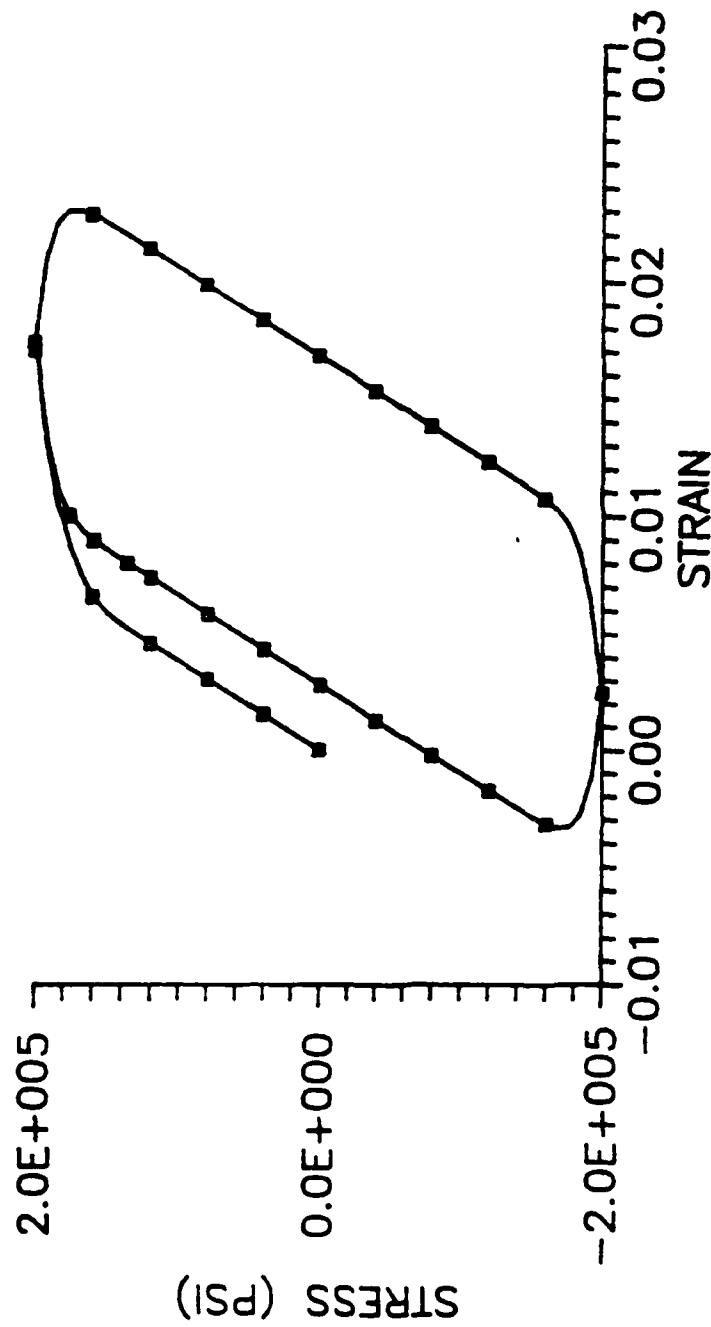
Frequency = 10 cpm  
 Peak stress =  $\pm$  200 KSI  
 Dashed lines and symbols show validated model results.  
 Solid lines show FINELS program predictions.

Figure 3. IN 100 Time Convergence Study,  $DT = 0.01$  sec.



Frequency = 10 cpm  
 Peak stress = +/- 200 KSI  
 Dashed lines and symbols show validated model results.  
 Solid lines show FINELS program predictions.

Figure 4. IN 100 Time Convergence Study,  $DT = 0.005$  sec.



Frequency = 10 cpm  
 Peak stress = +/- 200 KSI  
 Dashed lines and symbols show validated model results.  
 Solid lines show FINELS program predictions.

Figure 5. IN 100 Time Convergence Study,  $DT = 0.001$  sec.

inaccuracies or ratcheting did not occur when the time step used was smaller than 0.009 seconds.

A similar time convergence study was performed for Inconel 718 at 1200 F subjected to uniaxial cyclic strains of  $\pm 0.008$  peak values applied at a frequency of 10 cpm. In this case, cyclic strain was analyzed due to the model's inadequate cyclic stress prediction. The time steps used were 0.1 seconds, 0.05 seconds, 0.01 seconds, and 0.005 seconds. The results for each time step size are shown in Figures 6 through 8.

Under cyclic strain, no ratcheting is produced. However, convergence was noted since the stress-strain curve for  $dt = 0.005$  seconds was closely matched by that for  $dt = 0.01$  seconds and less closely matched as the time step sizes increased.

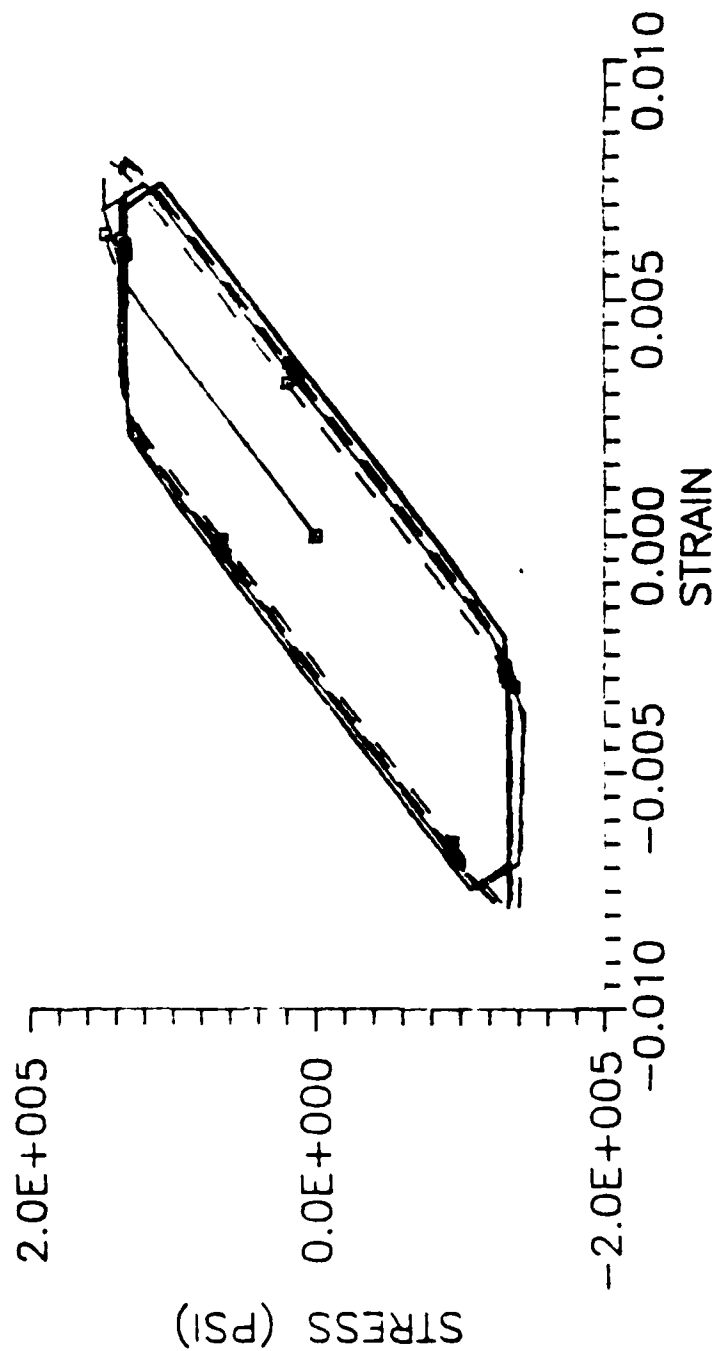
The maximum allowable time step size can be calculated using Equation 26. For a peak stress of approximately 150 KSI it is

$$dt_{\max} = 0.006 \text{ seconds}$$

Therefore steadily increasing divergence is expected for  $dt = 0.01$  seconds, 0.05 seconds, and 0.1 seconds, respectively.

For this investigation, Cormeau's method for determining the maximum allowable time step for numerical stability during Euler time integration was found to be valid for the Bodner-Partom model as well as for the other viscoplasticity models used. However, if conditions other than the ones used in this investigation are to be modelled, a limited time convergence study may be desirable to confirm the accuracy of the model.

Accuracy is also affected by the number of time steps per cycle of applied stress or strain. No systematic attempt was made to calculate the minimum number of time steps per cycle necessary for accurate results. However, at

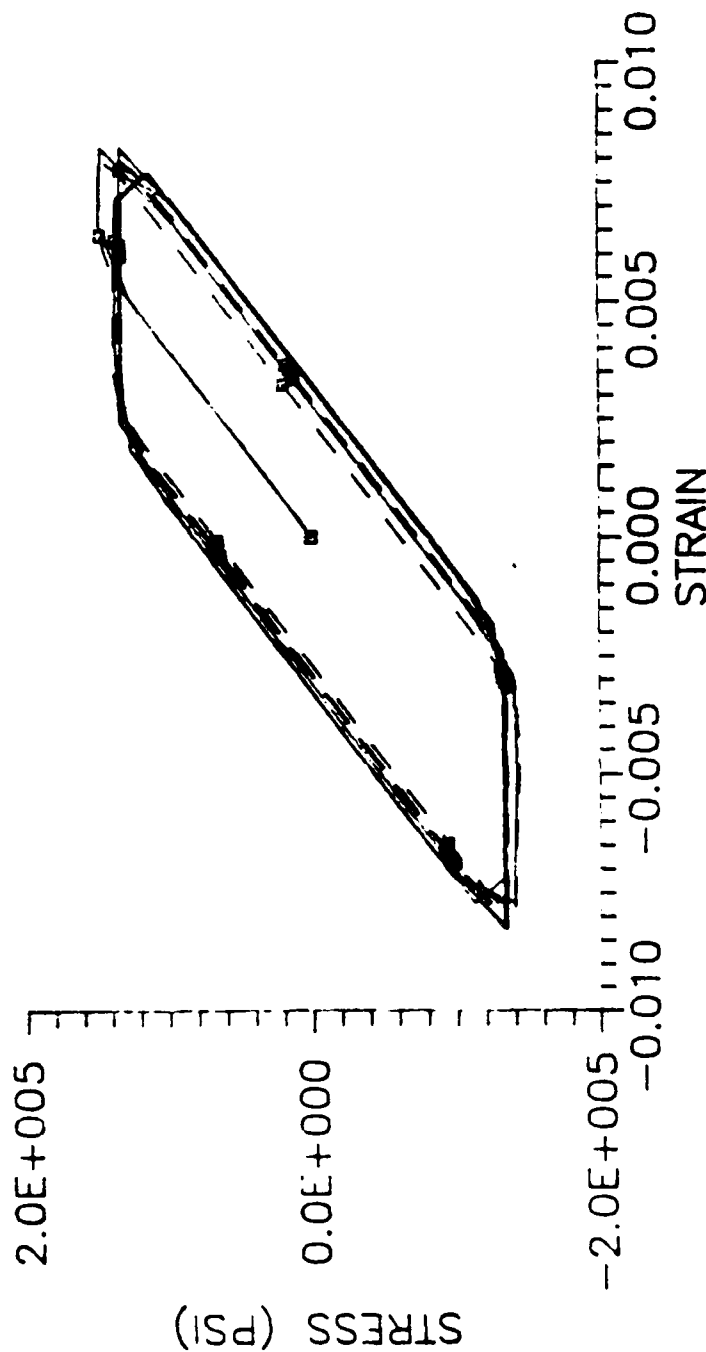


Frequency = 10 cpm  
Peak strain =  $\pm 0.008$

Dashed lines and symbols show  
stable results ( $DT = 0.005$  sec).  
Solid lines show predictions for  
time step  $DT = 0.1$  sec.

Figure 6. IN 718 Time Convergence Study,  $DT = 0.1$  sec.

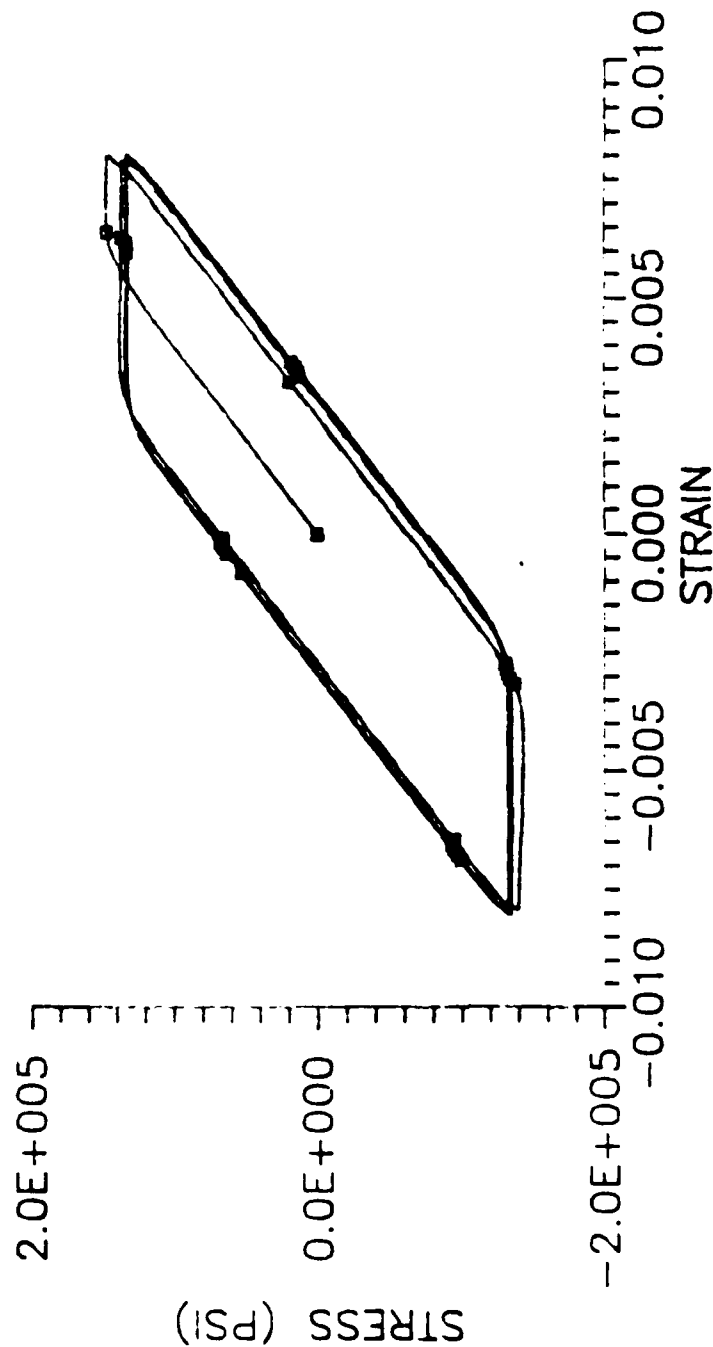




Frequency = 10 cpm  
Peak strain = +/- 0.008

Dashed lines and symbols show  
stable results ( $DT \approx 0.005$  sec).  
Solid lines show predictions for  
time step  $DT = 0.05$  sec.

Figure 7. IN 718 Time Convergence Study,  $DT = 0.05$  sec.



Frequency = 10 cpm  
Peak strain = +/- 0.008

Dashed lines and symbols show  
stable results ( $DT = 0.005$  sec).  
Solid lines show predictions for  
time step  $DT = 0.01$  sec.

Figure 8. IN 718 Time Convergence Study,  $DT = 0.01$  sec.

high stress, the maximum time steps allowed by Equations 24 through 26 are very small compared to the cyclic period. This placed a lower limit upon the number of time steps which occurred during each cycle. It was found that this resulted in a sufficient number of time steps per cycle to provide accurate results. The time step sizes used for predictions at the highest stress levels were therefore used for lower stress levels as well.

FINELS was also used to duplicate the results obtained by Hinnerichs and Palazotto (Ref 15) for a three bar linkage undergoing viscoplasticity and creep. This is discussed in Appendix B.

#### **Comparison of FINELS Output with Test Data**

FINELS' accuracy was further confirmed by duplicating the results Stouffer (Ref 11) obtained when determining the Bodner-Partom material constants for IN 100 at 1350 F from uniaxial tensile and creep test data (See Appendix A). FINELS' results matched Stouffer's; the stresses and strains calculated using the Bodner-Partom model were in close agreement with tensile test data, but showed the same discrepancies as Stouffer's results when compared to creep test data.

Using Stouffer's constants for IN 100, the Bodner-Partom model calculates creep strain rates which at low stress levels are initially too low, and which at higher stress levels are initially too high, although in all cases the creep strain rate eventually stabilizes at the correct value. This behavior is directly related to the thermal recovery of hardening defined in Equation 8, which controls the rate at which the parameter  $Z$  evolves. In this case,  $Z$  does not evolve rapidly enough to allow creep strain rate to stabilize quickly. If  $Z$  is initially too high, the creep rate will initially be too low until  $Z$  evolves to its proper value. Similarly, if  $Z$  is initially too low, the creep rate will initially be too high. This will lead to cumulative error over time if the rate at which  $Z$  evolves is too slow.

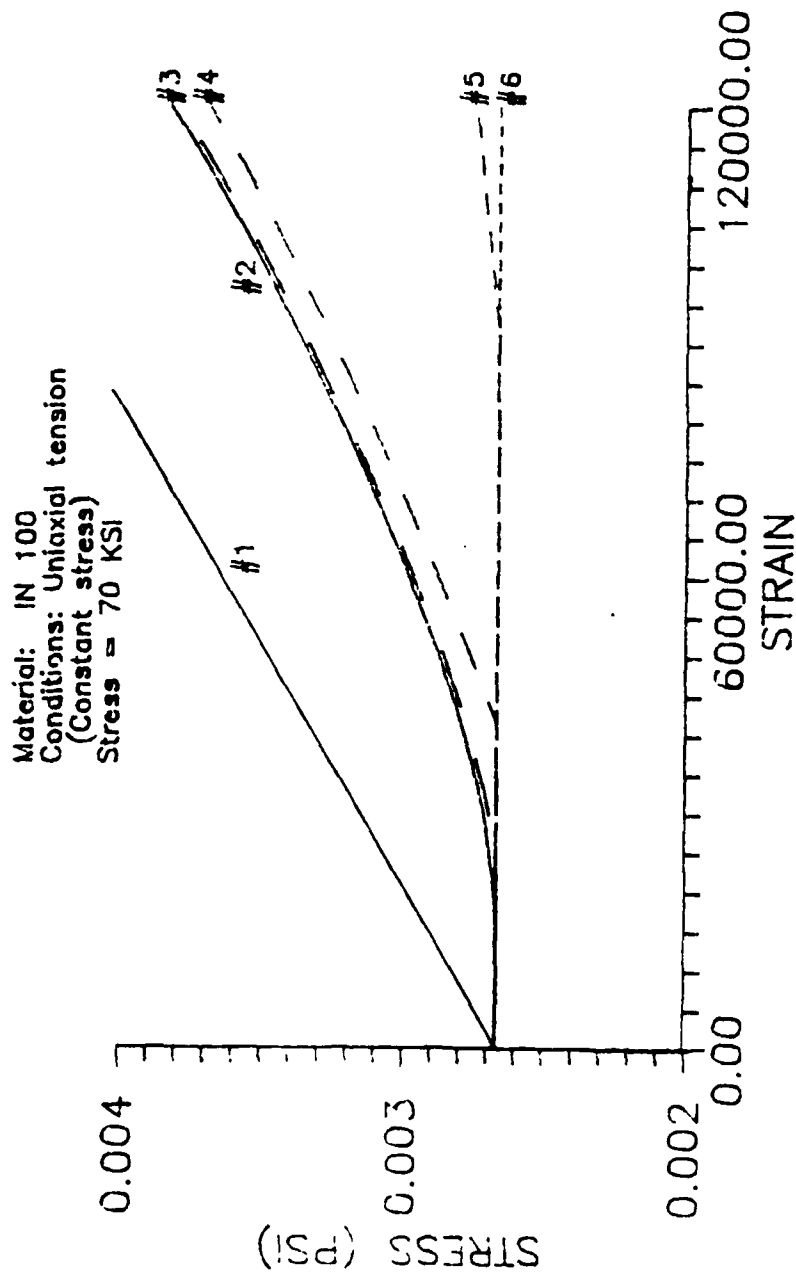
Stouffer points out that the material constants related to thermal recovery,  $A$ ,  $r$ , and  $Z_0$ , are not well-defined for IN 100 due to the large scatter in the creep test data. This behavior is therefore a potential source for cumulative error when modelling IN 100 in situations where significant creep will occur.

**Computer Accuracy.** It was initially thought that the accuracy of the computer may have caused the inaccuracy for low stress levels. The VAX 11/780 upon which FINELS was run reads any number less than  $1.0 \times 10^{-38}$  as zero. Since inelastic strain rate contributes to the evolution rate of  $Z$ , and since the initial inelastic strain rate is small for low stress, it was thought that the computer may have been causing errors by reading the strain rate contribution as zero.

Confirmation was attempted by modifying FINELS to change the value of the number read by the computer as zero. It was thought that artificially altering the computer's accuracy in this manner would further slow the rate at which  $Z$  evolves, thereby increasing the time required for the creep rate to stabilize at its proper value.

It was found that this was not the primary cause of the slow creep rate evolution, since an increase of the "zero" value from  $1.0 \times 10^{-38}$  to  $1.0 \times 10^{-26}$  did not cause significant differences in the predictions (See Figure 9).

It was also found that further increases in "zero" value to  $1.0 \times 10^{-24}$ ,  $1.0 \times 10^{-23}$ , and  $1.0 \times 10^{-20}$  did significantly affect the accuracy of the predictions, however (See Figure 9). This is not due to inaccuracies in the evolution rates of the internal variables. Rather, it is because the exponential term used in Equation 2 to calculate the viscoplastic strain rate has a value which is very small (on the order of  $1.0 \times 10^{-23}$ ) under these conditions even when the internal state variable reaches its steady-state value. This represents a source of progressive error when performing creep predictions using computer systems whose accuracy is less than that of the VAX 11-780.



KEY: 1. Actual Material Behavior (Ref 10)  
2. Prediction, 'zero' =  $1.0e-38$   
3. Prediction, 'zero' =  $1.0e-25$   
( 'zero' refers to quantity below which machine reads numbers as zero)  
4. Prediction, 'zero' =  $1.0e-24$   
5. Prediction, 'zero' =  $1.0e-23$   
6. Prediction, 'zero' =  $1.0e-20$

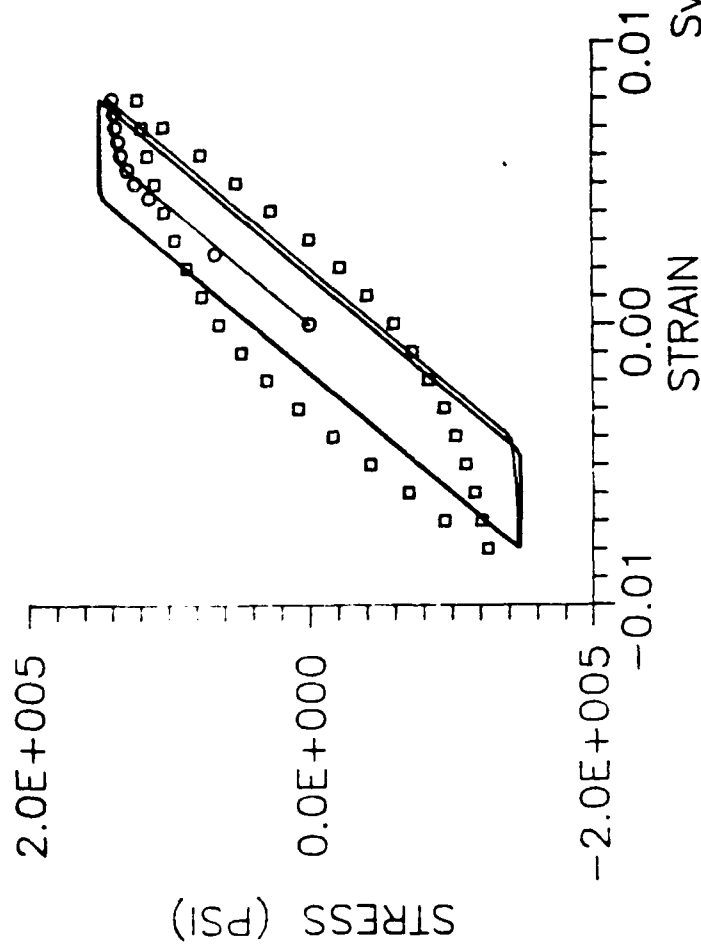
Figure 9. Effect of Machine Accuracy upon Creep Predictions.

### Frequency Response of the Bodner-Partom Model

FINELS was used to predict the stress-strain response of uniaxial tensile test specimens subjected to cyclic stresses and strains comprising a range of frequencies and amplitudes (See Table III). Inconel 718 at 1200 F was selected as the material to be modelled since extensive cyclic tensile test data exists to aid in verifying the model's accuracy. The Bodner-Partom material constants initially selected were those developed by Beaman (Ref 8) and used by Mercer (Ref 9) for Inconel 718 (See Table I).

Table III Matrix of Predicted Results Bodner-Partom Model Uniaxial Cyclic Stress							
Peak Stress (KSI)	Frequency (cpm)						
	100	10	6.7*	1	0.1	0.01	0.001
150	E	I	-	I	I	I	I
120	E	E	E	I	I	I	I
100	E	E	-	E	E	E	E
70	E	E	-	E	E	E	E
* Comparison with test data							
KEY: I = Instability VP = Viscoplastic Response C = Creep Response E = Elastic Response (Little or no viscoplasticity or creep)							

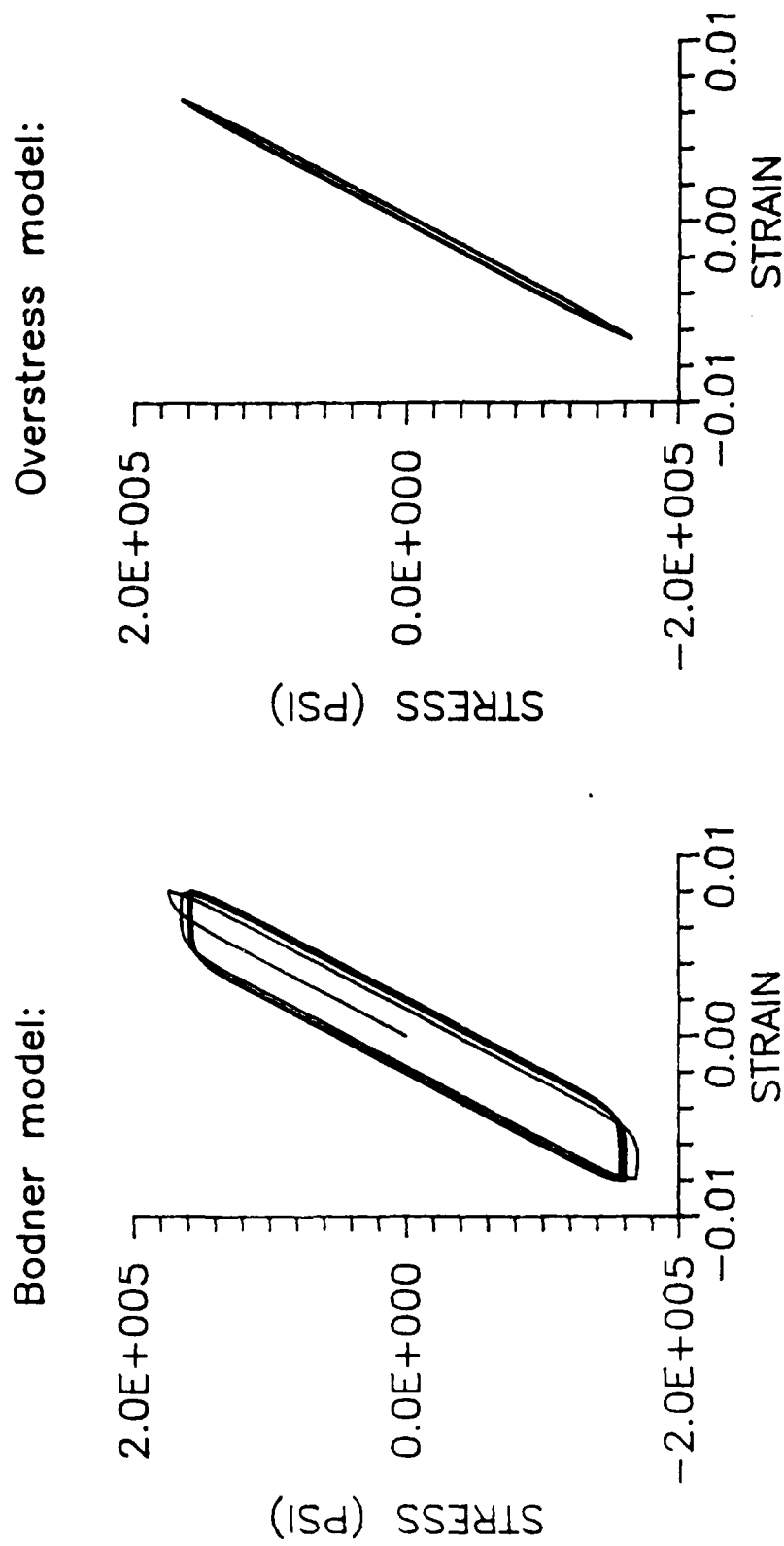
After the first few runs it became apparent that the material constants used did not properly portray the material's behavior (See Figure 10). The material constants portray a strain-hardening material, while the test data indicate that strain softening actually occurs, i.e. when a cyclic strain is applied the material reaches a high peak stress during the first cycle and attains lower peak stresses during following cycles (See Figures 11 through 16), while during cyclic stress it shows gradually increasing peak strains from one cycle to the next (See Figure 17). Revised material constants were clearly required.



Symbols show test data:  
 Circles = initial loading  
 Squares = steady state  
 Lines show model predictions.

Frequency = 10 cpm.  
 Peak strain =  $\pm 0.008$

Figure 10. IN 718 Prediction (Table 1 Material Properties, Initial Set).

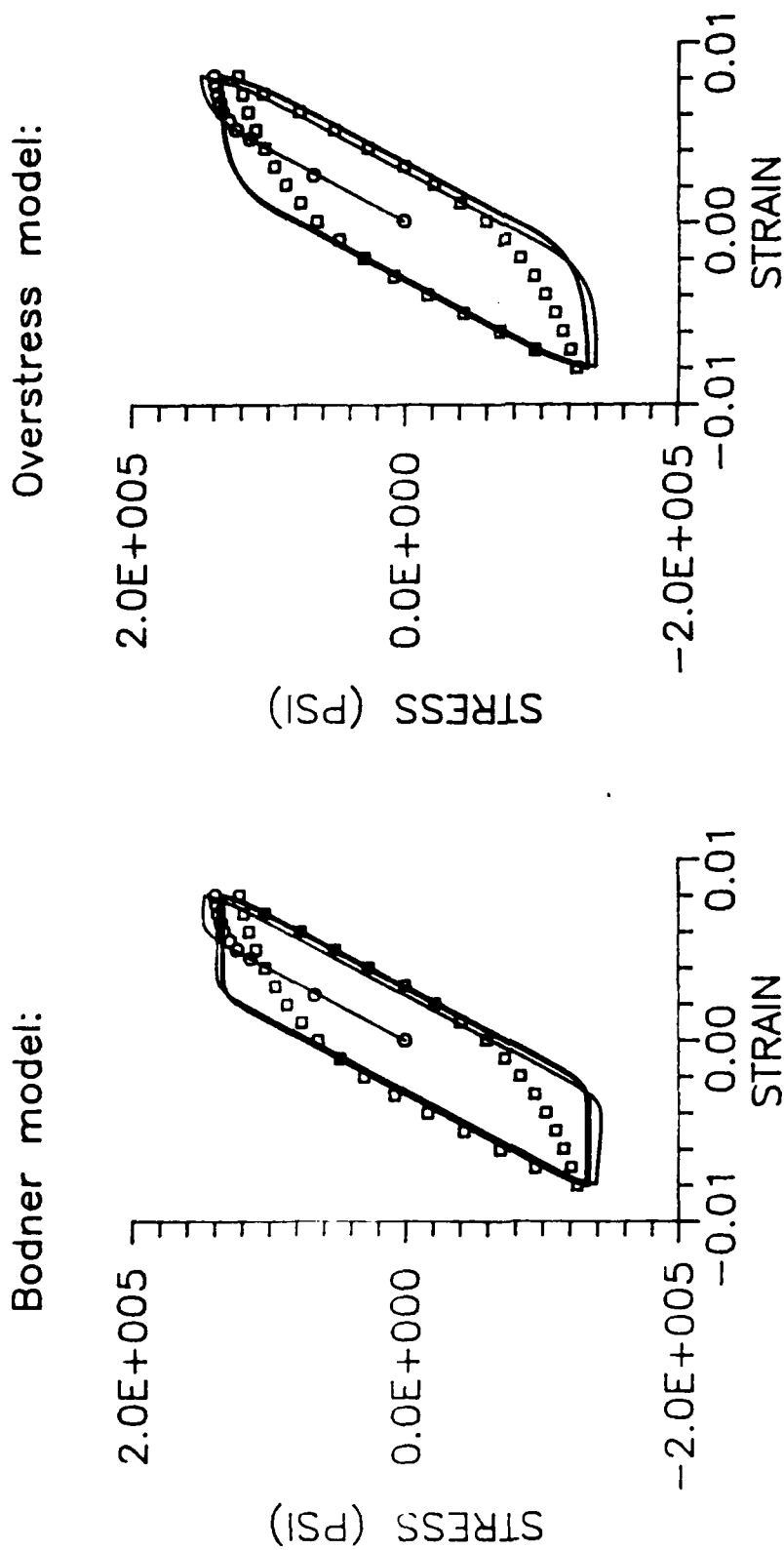


Frequency = 100 cpm  
Peak strain =  $\pm 0.008$

Lines show model predictions.

Figure 11. Uniaxial Cyclic Strain Predictions (100 cpm).



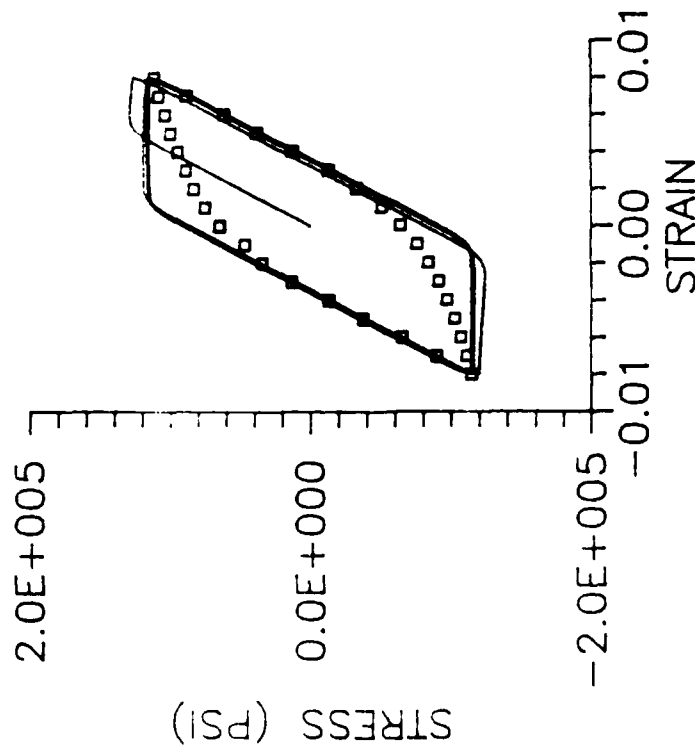


Frequency = 10 cpm  
 Peak strain =  $\pm 0.008$

Symbols show test data:  
 Circles = initial loading  
 Squares = steady state  
 Lines show model predictions.

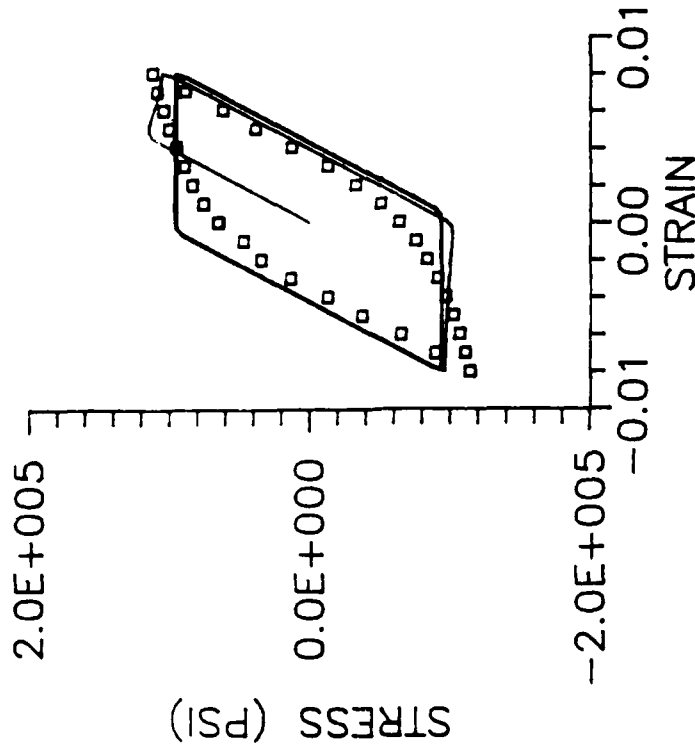
Figure 12. Uniaxial Cyclic Strain Predictions (10 cpm).

Bodner model:



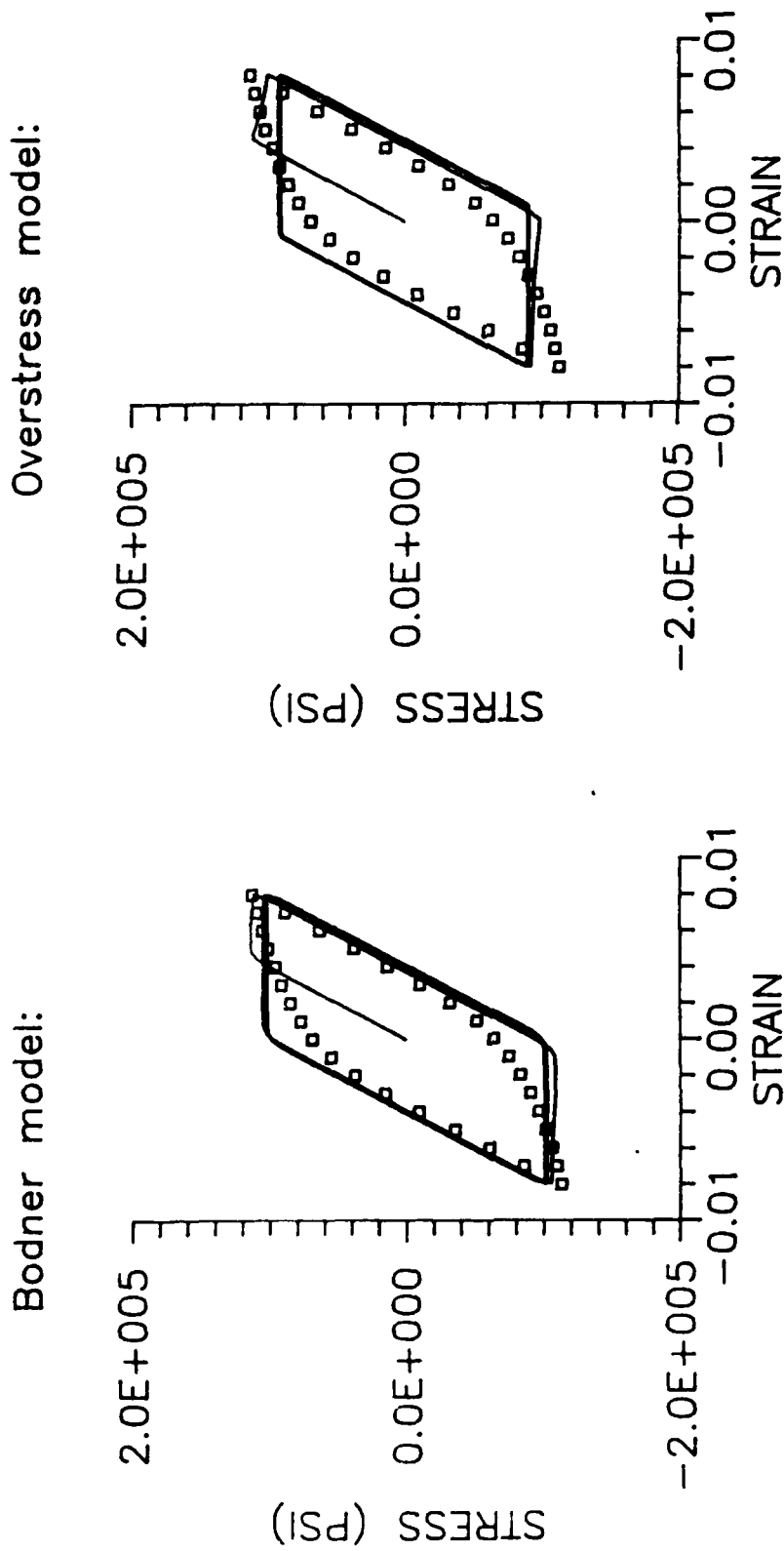
Frequency = 1 cpm  
Peak strain =  $\pm 0.008$

Overstress model:



Symbols show test data:  
Squares show steady state  
Lines show model predictions.

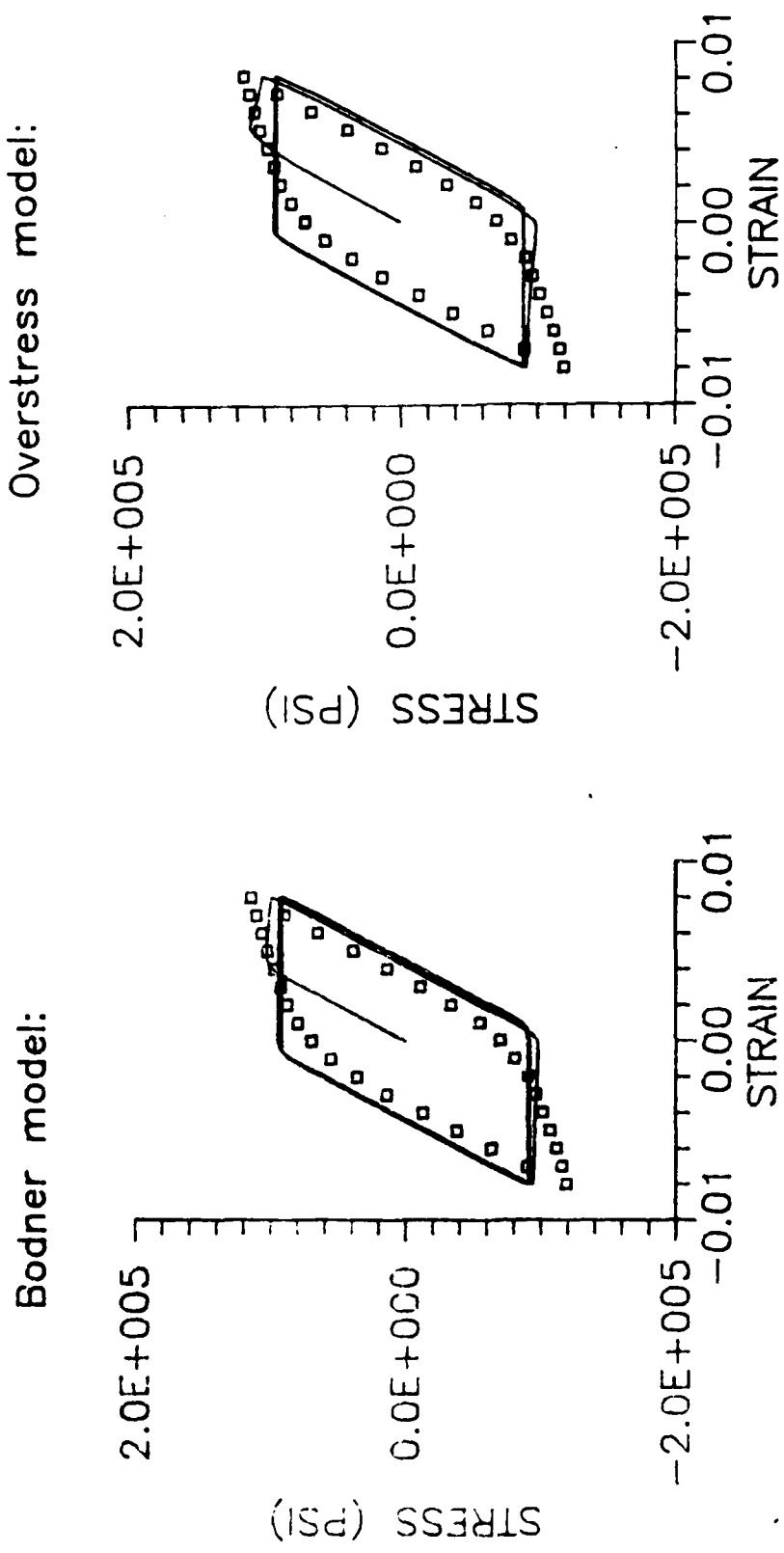
Figure 13. Uniaxial Cyclic Strain Predictions (1 cpm).



Frequency = 0.1 cpm  
 Peak strain = +/- 0.008

Symbols show test data:  
 Squares = steady state  
 Lines show model predictions.

Figure 14. Uniaxial Cyclic Strain Predictions (0.1 cpm).

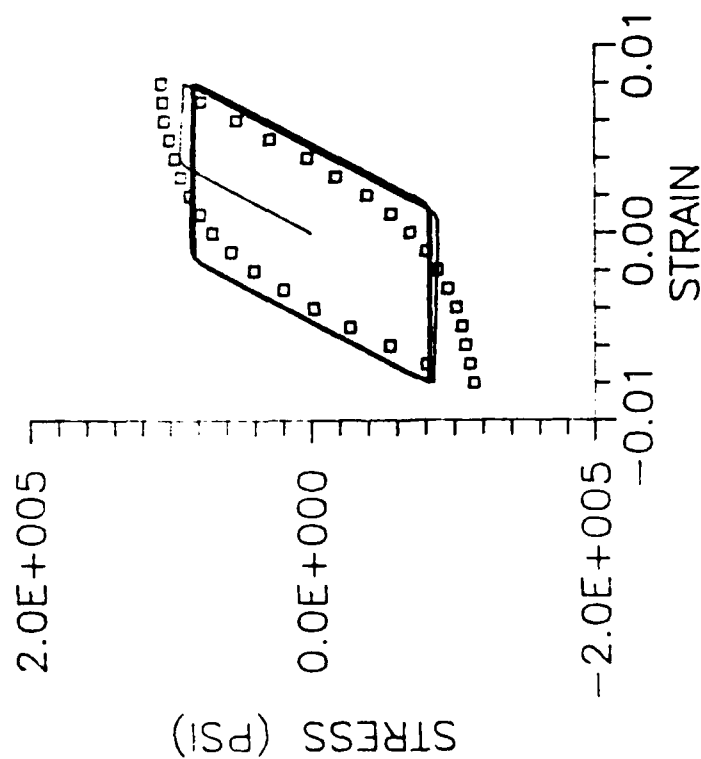


Frequency = 0.01 cpm  
 Peak strain = +/- 0.008

Symbols show test data:  
 Squares = steady state  
 Lines show model predictions.

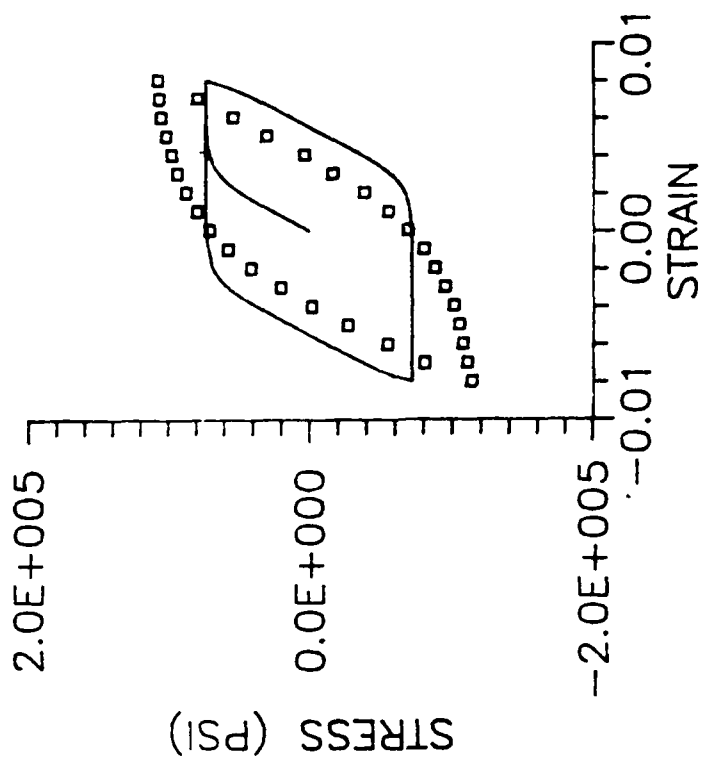
Figure 15. Uniaxial Cyclic Strain Prediction (0.01 CPM)

Bodner model:



Frequency = 0.001 cpm  
Peak strain = +/- 0.008

Overstress model:

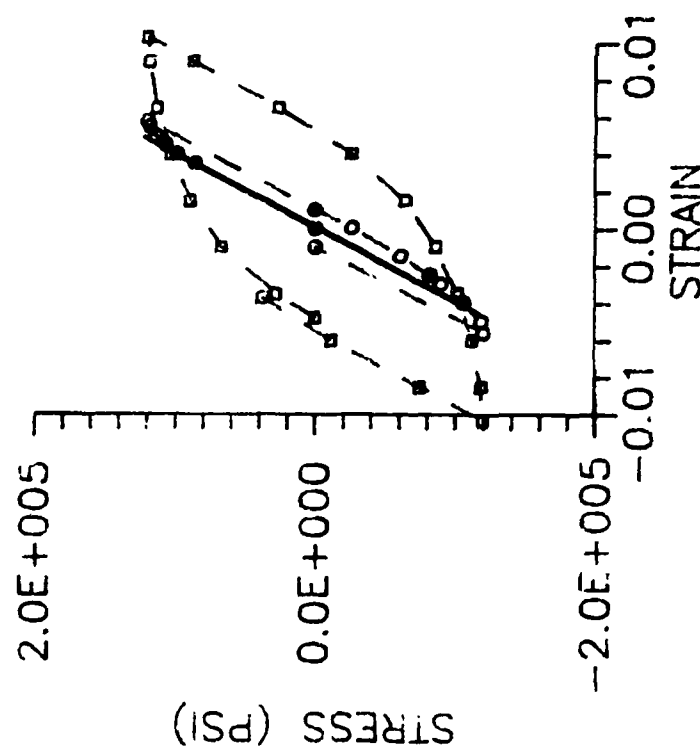


Symbols show test data:  
Squares = steady state

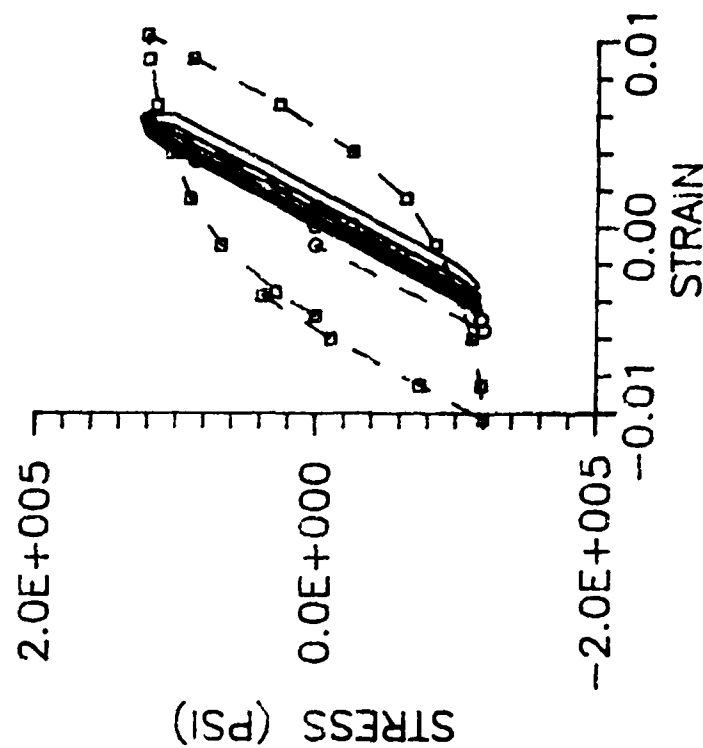
Lines show model predictions.

Figure 16. Uniaxial Cyclic Strain Prediction (0.001 CPM)

Bodner model:



Overstress model:



Frequency = 6.7 cpm  
Peak stress = +/- 120 KSI

Dashed lines & symbols show test data:  
Circles = first cycle  
Squares = fifth cycle  
Solid lines show model predictions.

Figure 17. Uniaxial Cyclic Stress Prediction (120 KSI, 6.7 CPM)

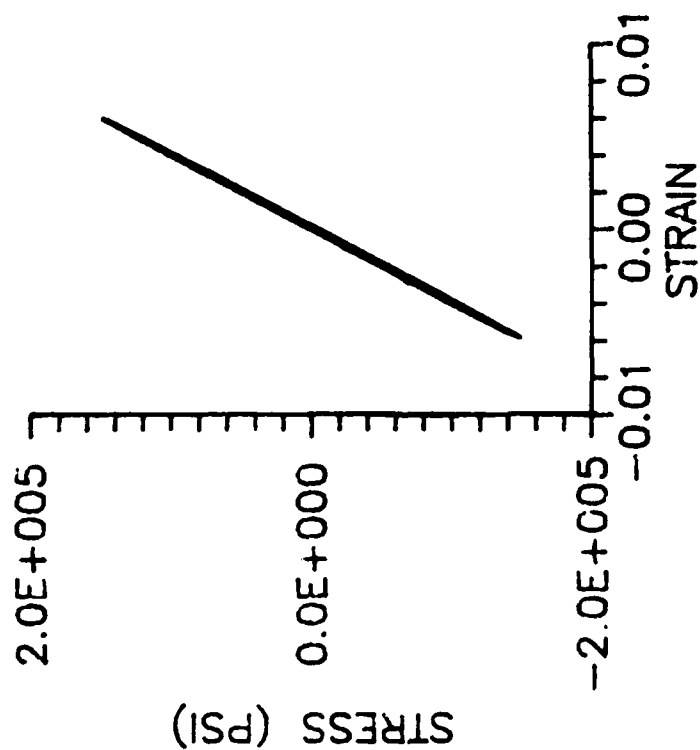
The revised Bodner-Partom material constants were calculated from Inconel 718 cyclic test data using the methods described by Stouffer (See Table I). When predicting strain-control behavior, they were found to portray the material's viscoplastic behavior reasonably well over the range of frequencies modelled (See Figs. 11 through 16). However, as with the original material constants, they produced stress-strain curves with sharply defined yielding points, rather than the smooth stress-strain curves produced by the test data. This is due to the exponential relationship between stress and viscoplastic strain rate assumed in the Bodner-Partom model (See Equations 1 through 4).

Using the new constants, the Bodner-Partom model did not predict stress-control behavior adequately. No appreciable viscoplasticity was predicted although the test data indicate that considerable viscoplasticity occurs under the conditions modelled (See Figures 17 through 19).

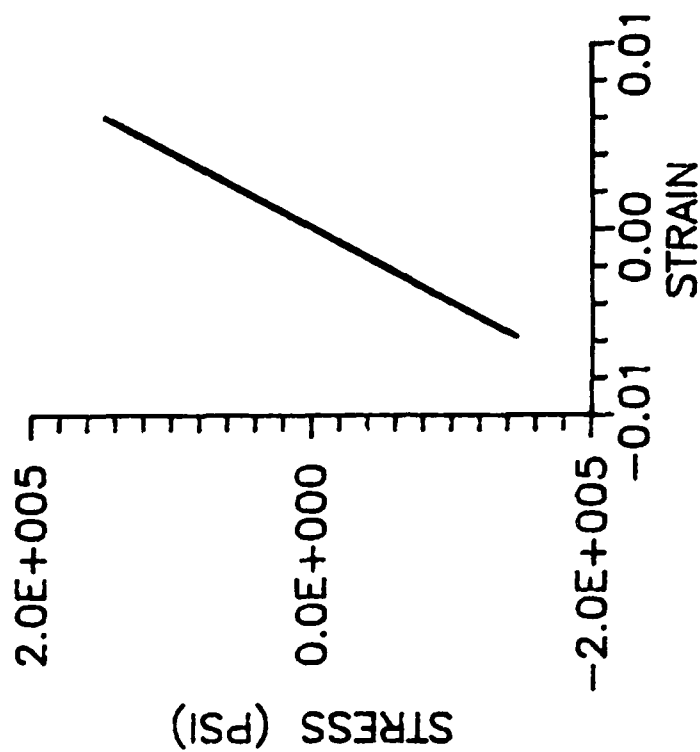
It was also found that when strain softening behavior was closely modelled, pure creep was not adequately portrayed. This is because the model does not allow  $Z$  to drop to a low enough value for significant creep to occur; in Equation 5, when  $Z_0$  is greater than  $Z_1$ ,  $Z_1$  becomes the lower limit for  $Z$ . Thermal recovery of plastic work cannot cause  $Z$  to become less than  $Z_1$  in this case. It is possible that this could be corrected by proper selection of recovery constants; however, this was not attempted.

Under stress control, the model became unstable at high applied stresses and low frequencies. Instabilities occurred at frequencies of 10 cpm and lower for peak stresses of  $\pm 150$  KSI and at frequencies of 0.1 cpm and lower for peak stresses of  $\pm 120$  KSI. As applied peak stresses decreased, the range of frequencies in which instability occurred grew smaller. This is consistent with the stability requirements described by Equation 27. At high stress and low frequencies, the increments in state variable and its evolution rate during a given time

Bodner model:



Overstress model:



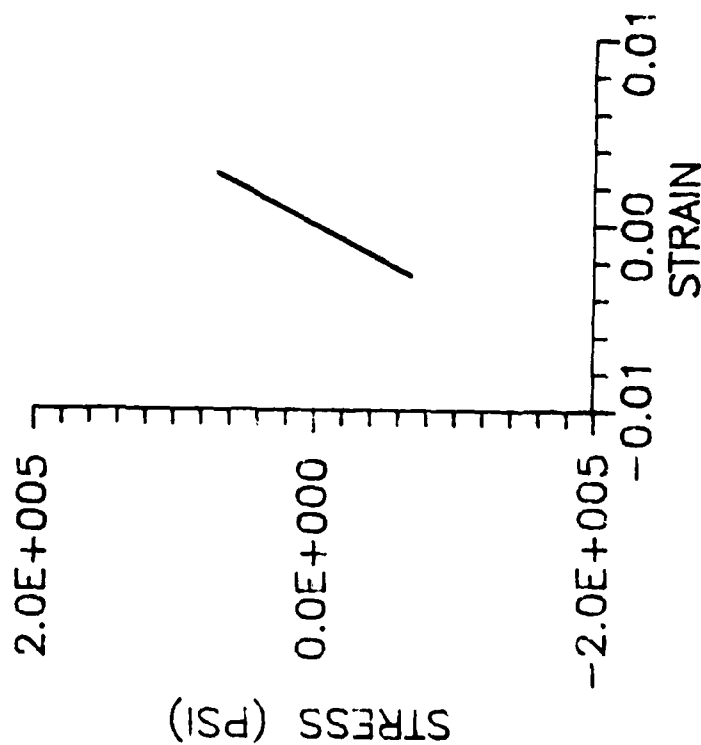
Frequency = 100 cpm  
Peak stress = +/- 150 KSI

Lines show model predictions.

Figure 18. Uniaxial Cyclic Stress Prediction (150 KSI, 100 CPM)

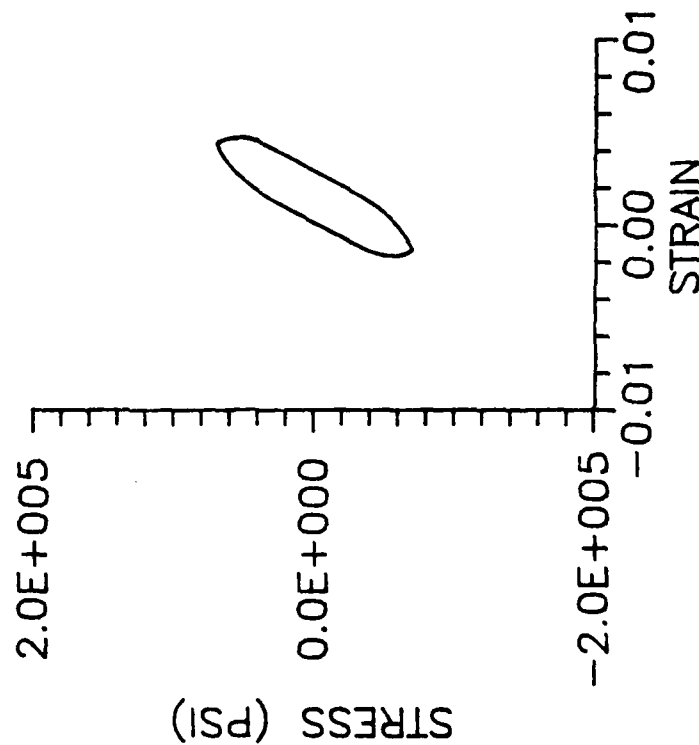


Bodner model:



Frequency = 0.001 cpm  
Peak stress = +/- 70 KSI

Overstress model:



Lines show model predictions.

Figure 19. Uniaxial Cyclic Stress Prediction (70 KSI, 0.001 CPM)

step become large, and for a strain softening material are sufficient to violate the requirements for stability.

Table III also shows the conditions for which the various types of Bodner-Partom model responses occurred.

#### Frequency Response of the Overstress/Norton Model

The same conditions were modelled (See Table IV) using a version of FINELS modified to use a combination of Overstress law to determine viscoplasticity and Norton's Law for Secondary Creep. Strain softening was modelled by making the yield stress in the Overstress equation a function of accumulated plastic strain:

$$\sigma_y = 100 \text{ KSI} (0.9 + 0.2 \exp[-m W_p]) \quad (28)$$

where  $W_p$  is the net plastic work and is given by

$$W_p = \int_0^t \sigma_{xx} \dot{\epsilon}^P_{xx} dt \quad (29)$$

or, during time step  $i$ ,

$$[W_p]^i = [W_p]^{i-1} + (\sigma_{xx}^i [\dot{\epsilon}^P_{xx}]^i) dt^i \quad (30)$$

Table IV Matrix of Predicted Results Overstress/Norton Model Uniaxial Cyclic Stress							
Peak Stress (KSI)	Frequency (cpm)						
	100	10	6.7*	1	0.1	0.01	0.001
150	E	E	-	I	I	I	I
120	E	E	VP	I	I	I	I
100	E	E	-	E	E	C	C
70	E	E	-	E	E	E	C
* Comparison with test data							
KEY:							
I = Instability							
VP = Viscoplastic Response							
C = Creep Response							
E = Elastic Response (Little or no viscoplasticity or creep)							

The Overstress/Norton model also yielded good predictions for strain-control behavior (See Figures 11 through 16). In fact, for high frequencies (1 cpm and higher), the Overstress/Norton model portrayed the material's behavior slightly more accurately than the Bodner-Partom model, since the Overstress/Norton model allows a smoother transition between creep and viscoplasticity at high stress/strain application rates. However, at lower frequencies the "on-off" nature of the Overstress law causes the stress-strain curve to assume the more squared-off shape characteristic of the Bodner-Partom model. This is because when the stress reaches the yield stress, the Overstress law causes the inelastic strain rates to increase by several orders of magnitude over a relatively small increment in stress.

At the highest frequency modelled, 100 cpm, a discrepancy was noted where the Overstress/Norton model predicted considerably less plastic strain than the Bodner-Partom model. In this case, although the Overstress/Norton model begins yielding at a lower stress, the Bodner-Partom model produces a higher viscoplastic strain rate once viscoplasticity begins.

The Overstress/Norton model did not adequately portray stress-control behavior (See Figures 17 through 19). Its results were similar to those of the Bodner-Partom model; although some viscoplasticity was shown at 120 KSI, the highest applied stress for which test data were available (See Figure 17), the predictions did not agree with the test data, while no appreciable viscoplasticity was shown in any other case (See Figure 18). At low stress, however, Norton's Law provided good predictions of creep response (See Figure 19).

It is possible that the Overstress law could be made to more closely match the material behavior by making the yield stress a function of total strain, in addition to plastic work, and by including recovery terms in a manner similar to that of the Bodner-Partom method. This is an area which requires further study.

In addition, the Overstress model was found to be unstable at high applied peak stress and low frequency during stress control. Instability occurred under the same conditions as for the Bodner-Partom model. This is also consistent with the stability criteria described by Equation 27. In this case, the yield stress evolves in a manner similar to that of the state variable  $Z$  in the Bodner-Partom model. It is therefore to be expected that instability should occur under approximately the same conditions (high stress, low frequency) as for the Bodner-Partom predictions.

Table IV also shows the conditions at which the various types of behavior occurred, i.e., instability, viscoplasticity, creep, and primarily elastic response.

Here it should be noted that the occurrence of instability indicates that viscoplasticity is occurring, since instability is triggered by evolution of the internal state variable (as shown in Equation 27), which in turn is brought about by the accumulation of viscoplastic strain.

#### **Cyclic Creep (IN 100)**

It has been noted that the isotropic strain-softening Bodner-Partom model is unable to model creep. This does not mean that the Bodner-Partom model cannot model creep under any conditions. In order to confirm that the Bodner-Partom model can model cyclic creep, a typical uniaxial cyclic creep response (100 KSI at 0.001 cpm) was modelled using the constants for IN 100 (See Table I). Since IN 100 is strain-hardening, the condition which prohibits calculation of creep in a strain-softening material does not occur.

The Bodner-Partom model results were compared to those of the Overstress/Norton model for the same conditions. In this case the material constants used were (Ref 10):

$$\sigma_Y = 130 \text{ KSI}$$

i.e., no viscoplasticity occurs since the maximum stress is only 100 KSI, and

$$\gamma_c = 3.7394 \times 10^{-60}$$

$$\beta = 10.64$$

The results are shown in Figure 20. Although the results of the two models do not match well, it can be seen that the Bodner-Partom model does calculate creep response. The inability to calculate creep does not occur when strain-hardening is modelled.

### Simulated Stress Concentration

Material behavior at a stress concentration was simulated by applying the Bodner-Partom model to a simple three-bar linkage subjected to a cyclic load applied at the central node. The applied loads comprised a range of frequencies and amplitudes (See Table V).

Table V Matrix of Predicted Results Bodner-Partom Model Simulated Stress Concentration						
Peak Force (KPS)	Frequency (cpm)					
	100	10	1	0.1	0.01	0.001
250	VP	VP	VP	VP	VP	VP
200	E	E	VP	VP	VP	VP
150	E	E	E	E	E	E
100	E	E	E	E	E	E
KEY:						
I = Instability						
VP = Viscoplastic Response						
C = Creep Response						
E = Elastic Response (Little or no viscoplasticity or creep)						

The three-bar linkage consists of three uniaxial bar elements as shown in Figure 21. Stress concentration is simulated by applying a force at the central node, oriented such that the highest proportion of the load is borne by Element #2. When this element begins yielding, it becomes effectively incapable of bearing further increases in internal load. Further increases in applied load must be

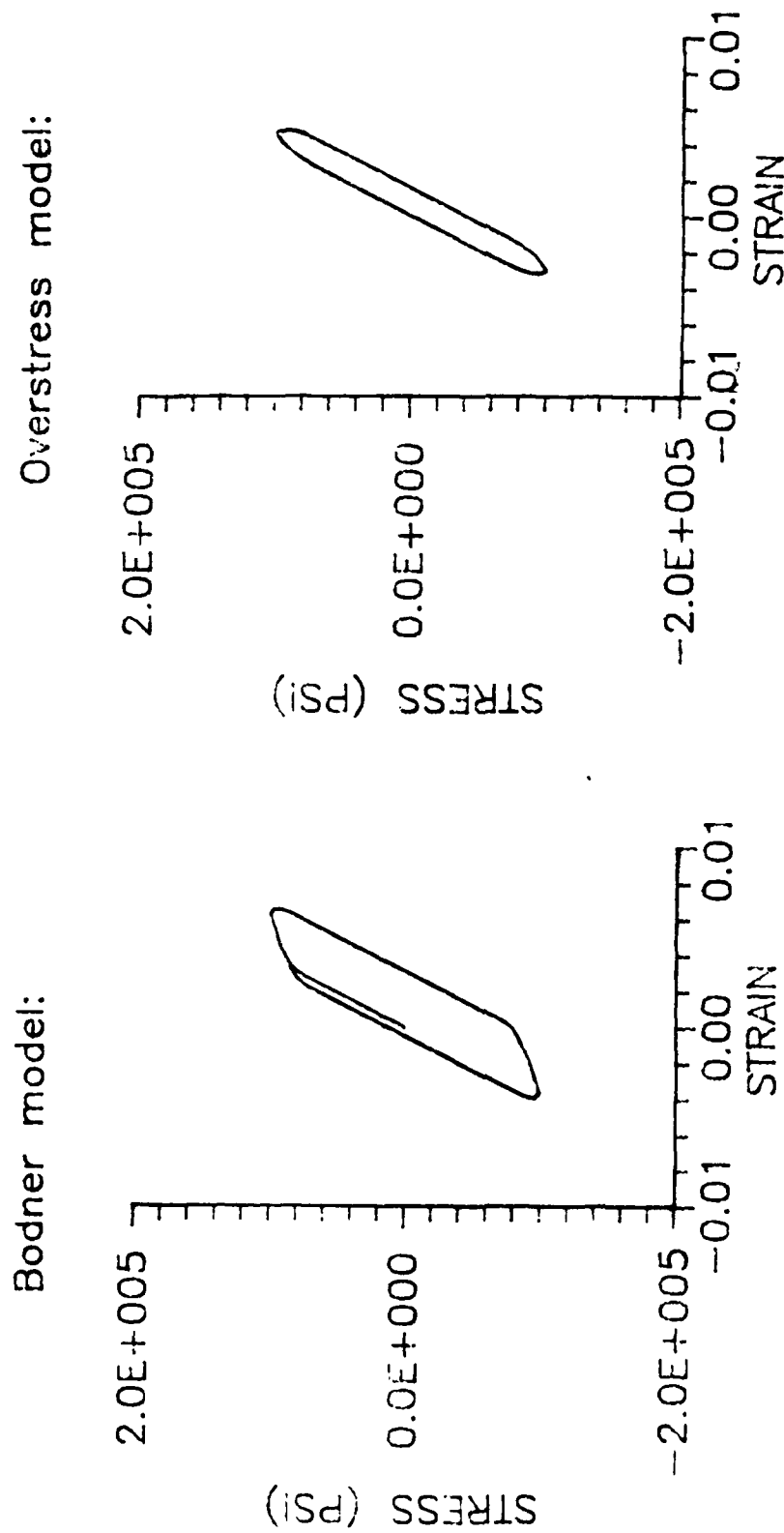


Figure 20. IN 100 Cyclic Stress Prediction (100 KSI, 0.001 CPM).

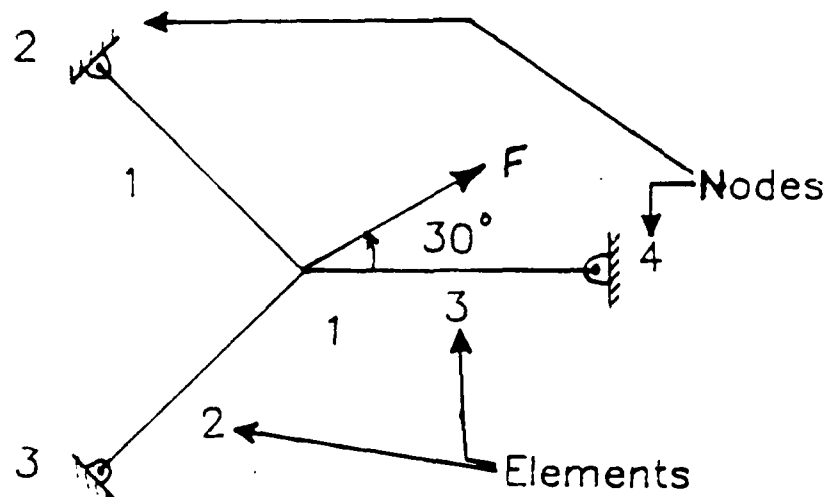


Figure 21. Simulated Stress Concentration  
(Three-Bar Linkage)

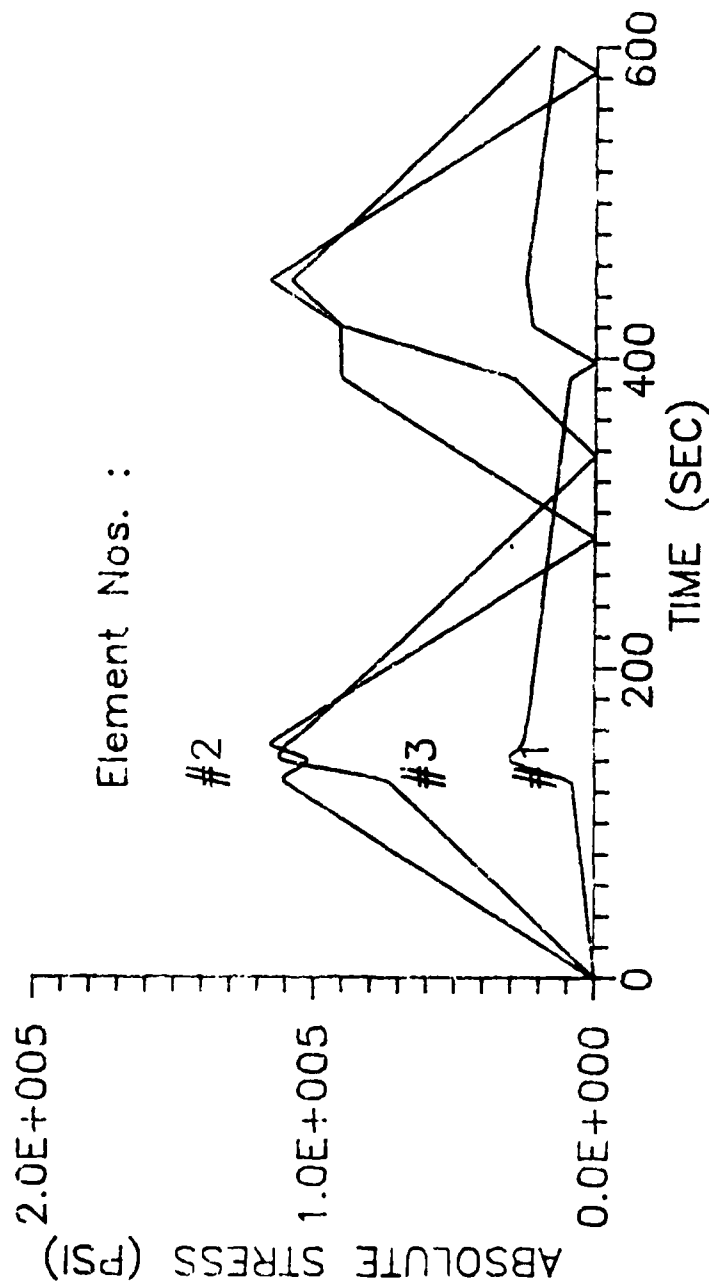
borne by the remaining two unyielded members. If the applied load is increased sufficiently, a second member will begin yielding, and finally the third. The model therefore shows how the inelastic behavior of one element affects the behavior of adjacent elements. In this manner, the model simulates the formation and growth of a plastic zone around a crack tip or other area of stress concentration in a two-dimensional model.

A plot of typical three-bar linkage behavior over time during cyclic applied stress is shown in Figure 22. In it, the points where load is transferred from one element to others due to viscoplastic response can clearly be seen.

In general, the behavior of the yielding elements (elements #2 and #3) was neither that of pure stress control nor that of pure strain control (see Figures 23 through 25). However, for applied forces of 200 KPS and 250 KPS peak value, the elements' behavior was that of pure stress control at the highest and lowest frequencies, where the peak stresses remained the same while the peak strains grew greater during each successive cycle. At intermediate frequencies, typically 10 cpm and 1 cpm, some behavior reminiscent of strain control was noted, i.e. high initial peak stress and lower peak stresses during subsequent loadings (See Figure 24).

The Bodner-Partom predictions were then compared to predictions obtained for the same conditions using the Overstress/Norton model (See Table VI). The Overstress/Norton model predicts behavior similar to that of the Bodner-Partom model although the results do not always match well. A comparison of results is shown in Figures 23 through 25.



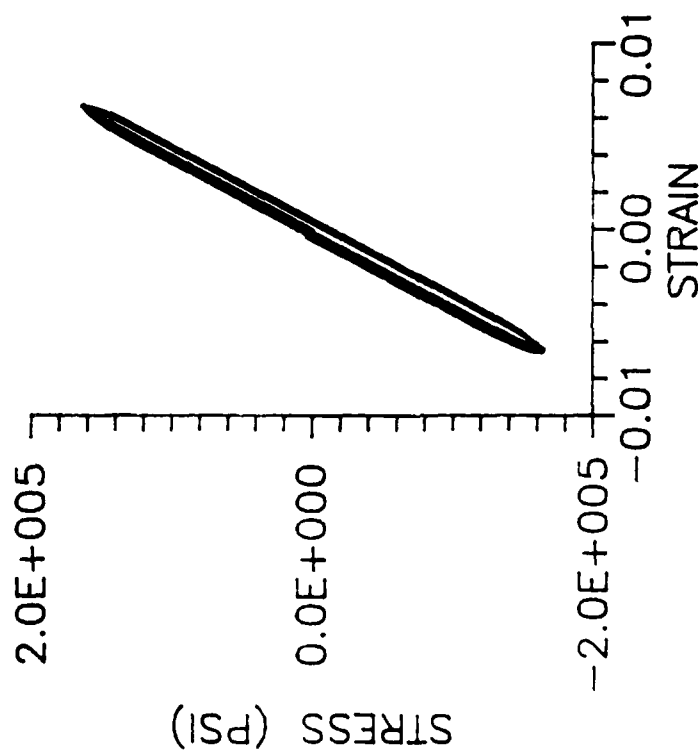


Material: IN 718  
 Conditions: Cyclic Applied Force  
 Peak Force =  $\pm 200$  KPS  
 Frequency = 0.1 cpm

Lines show model predictions.

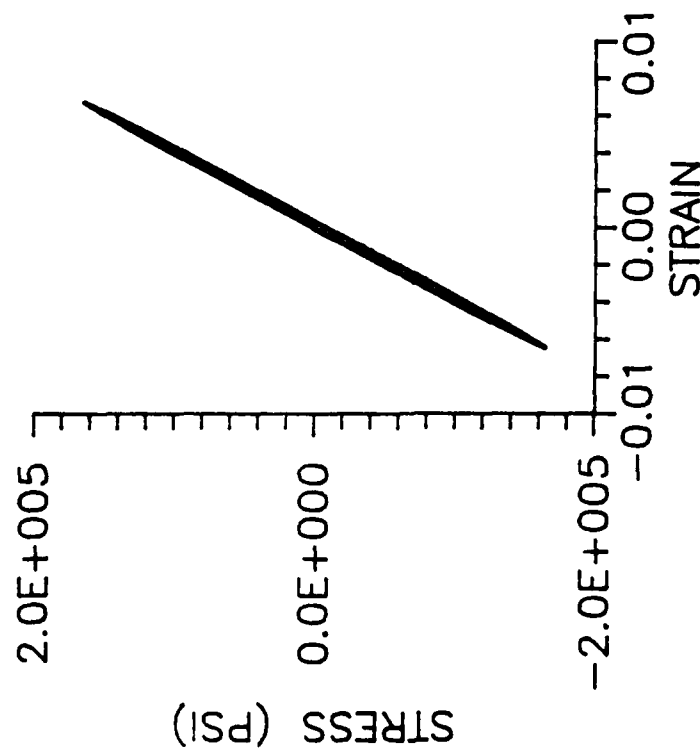
Figure 22. Stress vs. Time in a Viscoplastic Three-Bar Linkage

Bodner model:



Frequency = 100 cpm  
Peak force = +/- 250 KPS

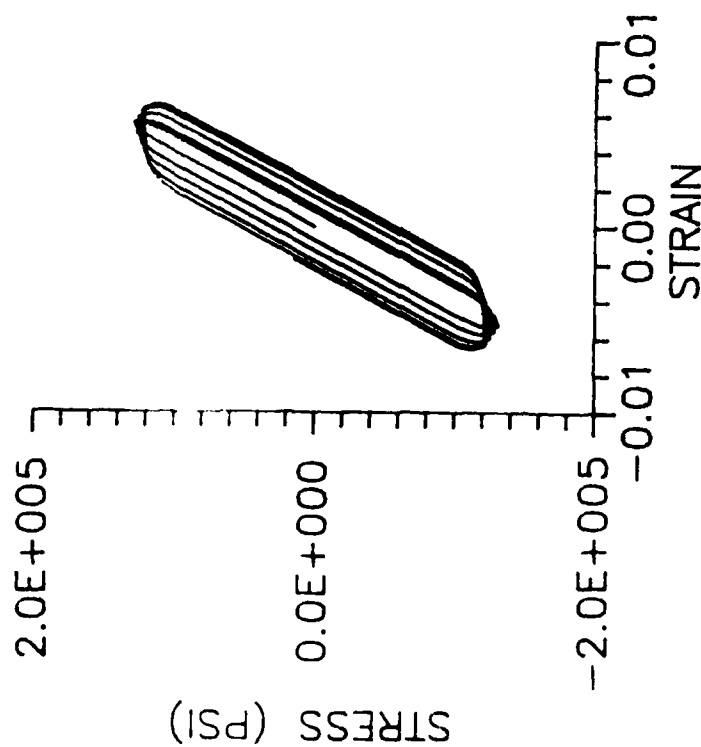
Overstress model:



Lines show model predictions.  
(Element #2 of three-bar linkage)

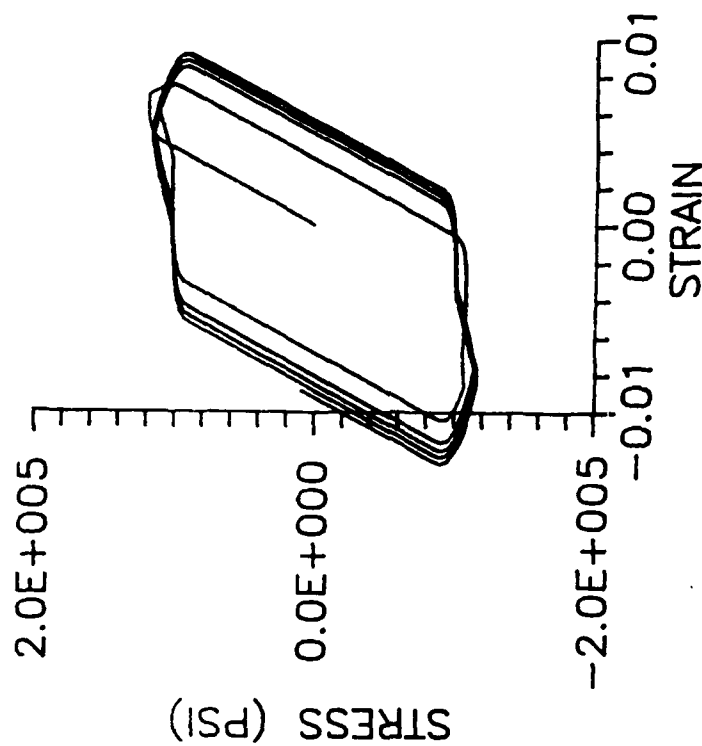
Figure 23. Stress Concentration Predictions (250 KPS, 100 CPM)

Bodner model:



Frequency = 1 cpm  
Peak force = +/- 200 KPS

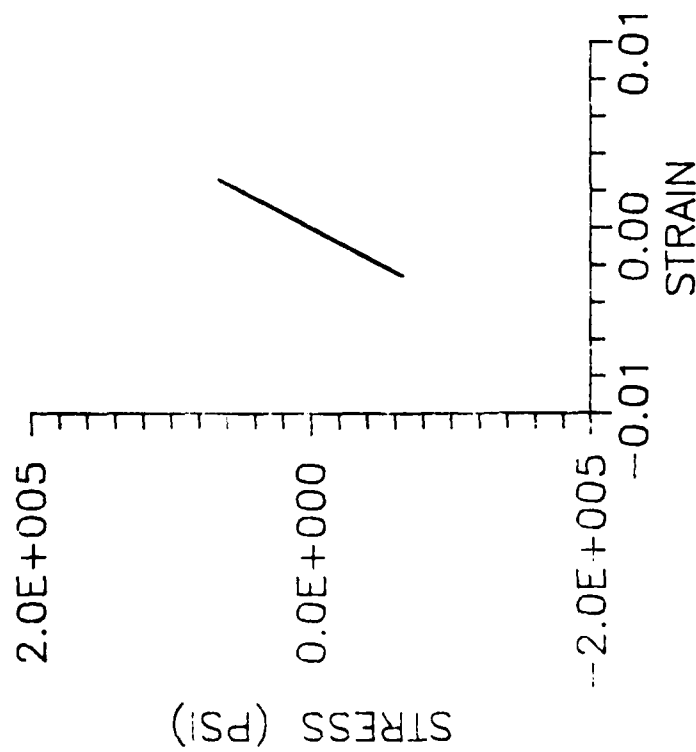
Overstress model:



Lines show model predictions.  
(Element #2 of three-bar linkage)

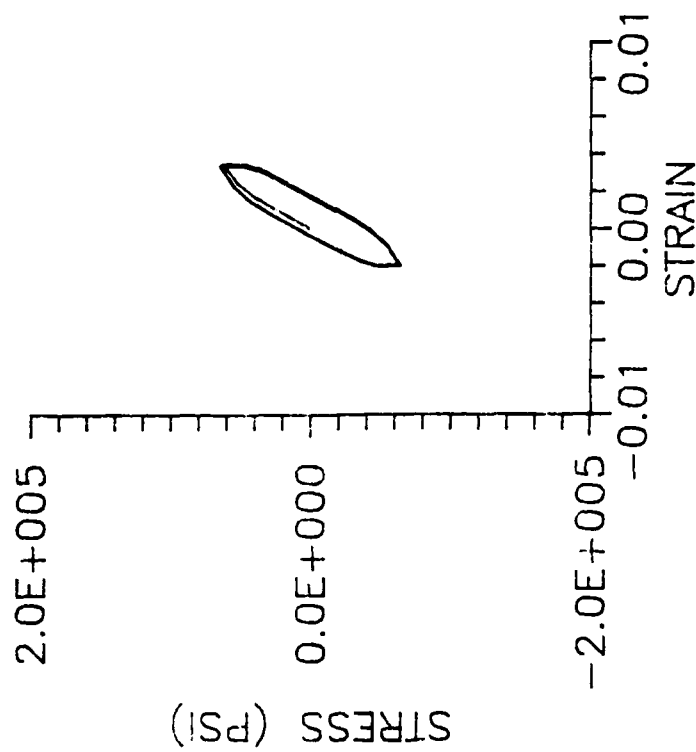
Figure 24. Stress Concentration Predictions (200 KPS, 1 CPM)

Bodner model:



Frequency = 0.001 cpm  
Peak force = +/- 100 KPS

Overstress model:



Lines show model predictions.  
(Element #2 of three-bar linkage)

Figure 25. Stress Concentration Predictions (100 KPS, 0.001 CPM)

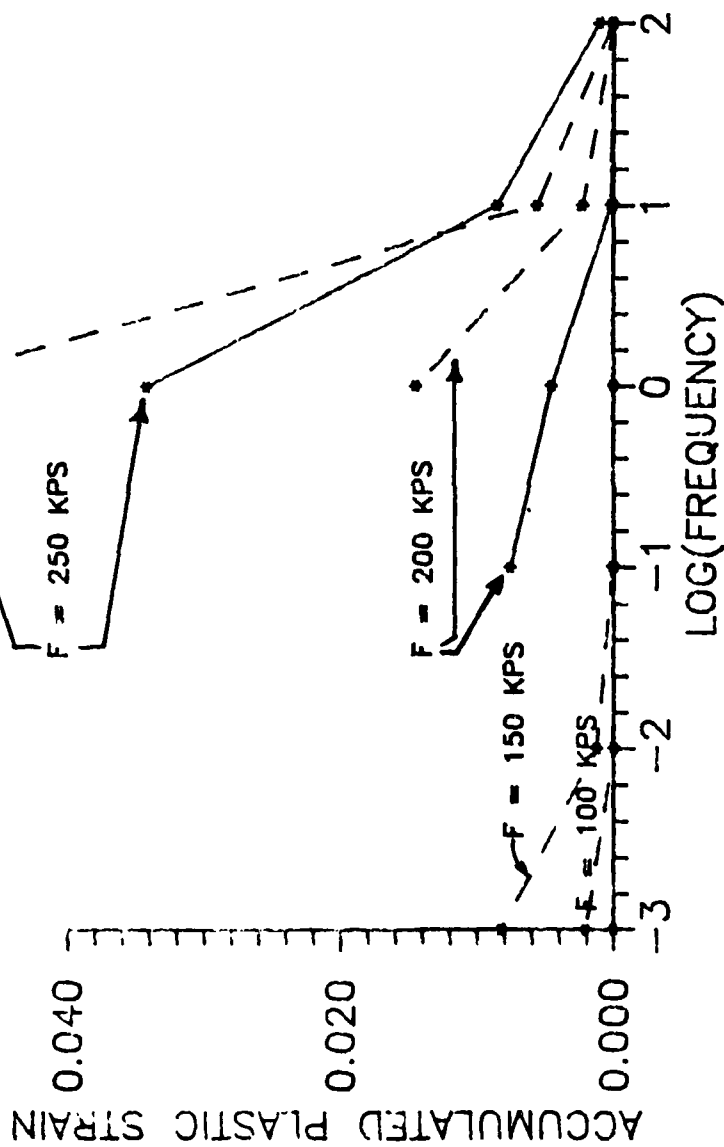
Table VI Matrix of Predicted Results Overstress/Norton Model Simulated Stress Concentration						
Peak Force (KPS)	Frequency (cpm)					
	100	10	1	0.1	0.01	0.001
250	E	VP	VP	VP	VP	VP
200	E	VP	VP	VP	VP	VP
150	E	E	E	E	C	C
100	E	E	E	E	E	C
KEY:						
I =Instability						
VP =Viscoplastic Response						
C =Creep Response						
E =Elastic Response (Little or no viscoplasticity or creep)						

The Overstress/Norton model predicted lower peak strains than those of the Bodner-Partom model for an applied force of 250 KPS (See Figure 23) while predicting higher peak strains for the corresponding frequencies when the force was 200 KPS (See Figure 24). In addition, at low applied forces and frequencies, the models' predictions diverged due to the Overstress/Norton's Law model's portrayal of creep and the Bodner-Partom model's previously noted inability to portray creep under these conditions (See Figure 25).

Instability did not occur. However, it must be noted that conditions of high applied stress and low frequency produce results which cannot be considered approximations of real-life results, since the strains produced by maintaining high loads for long periods are well past the rupture limit for the actual material. Also, the assumption of small deformations no longer applies. These predictions are therefore of questionable value for comparing the models' behavior.

Tables V and VI also show the conditions for which the various types of behavior occurred, i.e., viscoplasticity, creep, and primarily elastic response.

It is perhaps more informative to view the results in terms of accumulated inelastic strain vs. frequency as shown in Figure 26. This better shows the



Material: IN 718

Conditions: Cyclic Applied Force  
(Bar #2 of three-bar linkage)

Number of cycles = 5

— = Bodner-Partom model  
- - - = Overstress/Norton model

Figure 26. Plastic Strain vs. Frequency.

conditions for which a viscoplasticity model is necessary and those for which a simpler creep model or even a purely elastic model will suffice. At high stresses, inelastic strains are largely due to viscoplasticity. At low stresses, inelastic strains are largely due to creep. Where little or no inelastic strains occur, the response is primarily elastic.

## V. Conclusions

### Summary of Work Done

The cyclic behavior of the Bodner-Partom and combined Overstress/Norton's Law models were investigated over a range of frequencies and applied cyclic stresses and strains using the viscoplasticity prediction code FINELS developed for the purpose. For simplicity, only isotropic hardening was investigated, although kinematic hardening can also be modelled. FINELS was validated by comparison of its results with those of other codes and with cyclic and non-cyclic tensile and creep test data. Its ability to simulate stress concentration was tested by running the three-bar linkage problems formulated by Hinnerichs and Palazotto (Ref 15). FINELS was used to check the validity of Cormeau's (Ref 13) requirement for the maximum allowable time step size for a stable model. Uniaxial cyclic behavior was predicted for cyclic applied stresses and strains comprising a range of frequencies and amplitudes. Cyclic stress concentration behavior was predicted by modelling a three-bar linkage subjected to cyclic applied loads comprising a range of frequencies and amplitudes.

### Characteristics of the Bodner-Partom Model

**Frequency Response.** A viscoplasticity model is required to predict material behavior at high stresses (alternately, high strain rates) over a range of frequencies, and at intermediate stresses (or strain rates) at low frequencies (i.e., conditions corresponding to the upper right region of Tables III through VI), since these are the conditions near a crack tip for which, in real life, large viscoplastic strains will occur.

Both the Bodner-Partom model and the Overstress model can be used to predict viscoplastic response although their predicted results diverge somewhat at the highest applied stresses and strain rates.



Viscoplasticity models are not always required, however. For low stresses applied at low frequencies (the lower right region of Tables III through VI), the material's behavior is largely due to creep. In these cases, a simple model such as Norton's Law will adequately predict material behavior. For a strain-softening material, Norton's Law is actually preferable to the Bodner-Partom model due to the inability to predict creep using the isotropic strain-softening Bodner-Partom model under these conditions.

Also, for intermediate and low stresses at high frequencies (the lower left region of Tables III through VI), little or no viscoplasticity or creep will occur. Under these conditions, a purely elastic model will suffice for stress-strain prediction.

**Creep Behavior.** Inadequate creep test data prevents calculation of accurate recovery parameters. This in turn prevents accurate modelling of the evolution rate for  $Z$ . Although  $Z$  will eventually evolve to its appropriate value, a potentially large initial error will be introduced when creep predictions are made.

**Kinematic Hardening.** It appears that Inconel 718 shows significant kinematic hardening as well as isotropic hardening. Beaman (Ref 8) showed how the assumption of kinematic hardening produces results which match cyclic test data much more closely than results produced by purely isotropically hardening models. Lindholm, et al (Ref 7) also showed how the addition of kinematic hardening terms to  $Z$  allows the Bodner-Partom model to predict smoother, more accurate elastic-viscoplastic transition.

**Time Step Size.** Ratcheting and other cumulative errors can be eliminated by proper selection of the time step size. The time step size is critical to ensuring numerical stability of the Bodner-Partom model. Cormeau's approach to determining the maximum allowable time step was found to apply to the Bodner-Partom model as well as to others. When the time step exceeds this maximum

allowable value, cumulative error is introduced. Further increases in time step size cause ratcheting and eventually cause the model to "blow up" numerically.

**Strain Softening.** It has been previously noted that the Bodner-Partom model does not adequately portray creep when a strain-softening material such as Inconel 718 is modelled assuming isotropic hardening only. In Equation 5, when  $Z_0$  is greater than  $Z_1$ ,  $Z_1$  becomes the lower limit for  $Z$ . Thermal recovery of plastic work cannot cause  $Z$  to become less than  $Z_1$  in this case. The Bodner-Partom model can portray creep adequately when isotropic strain-hardening materials such as Inconel 100 are modelled.

**Numerical Instability.** Both models share a common limitation with all strain softening models: that of conditional stability. In this case, however, it is not of practical consequence since the conditions under which it occurs (high stresses and low frequencies; in this case, 10 cpm and lower at 150 KSI, 1 cpm and lower at 120 KSI) are those under which, in real life, the material would rupture.

#### **Simulated Stress Concentration.**

The behavior of Inconel 718 at a stress concentration when subject to cyclic remote stress or displacement is generally closer to that of pure stress control than to that of pure strain control, although under conditions of intermediate stress and frequency behavior similar to strain control can occur, namely high stresses during the first cycle and lower stresses during subsequent cycles.

## **VI. Recommendations**

### **Creep in a Strain Softening Material.**

The isotropic Bodner-Partom formulation for thermal recovery does not allow creep rate in a strain softening material. Alternate methods should be developed for determining the evolution of the state variable  $Z$  to allow it to evolve below the lower limit imposed upon it by Equation (5) for strain softening materials.

### **Kinematic Hardening.**

Kinematic hardening should be accounted for in all cyclic viscoplastic analyses involving high-temperature turbine materials.

### **Continued Investigation.**

The next step in an ongoing investigation should be to extend analysis to problems in two and three dimensions. The results of this investigation could be used to help identify the conditions at a crack tip for which each type of behavior (viscoplasticity, creep, elasticity) can be expected to occur.

## Bibliography

1. Military Standard, Engine Structural Integrity Program (ENSIP) MIL-STD-1783 (USAF), 30 November 1984.
2. Bodner, S.R., and Partom, Y., "Constitutive Equations for Elastic-Viscoplastic Strain Hardening Materials," *Journal of Applied Mechanics*, Trans. ASME, Vol. 42:385-389, 1975.
3. Estrin, Y., and Mecking, H., "An Extension of the Bodner-Partom Model of Plastic Deformation," *International Journal of Plasticity*, Vol. 2:73-85, 1986.
4. Walker, K.P., NASA-CR-165533, 1981.
5. Chaboche, J.L., and Cailletaud, G., "On the Calculation of Structures in Cyclic Plasticity or Viscoplasticity," *Computers and Structures*, Vol. 23(1):23-31, 1986.
6. Stickforth, J., "On Stress Relaxation, Creep, and Plastic Flow," *International Journal of Plasticity*, Vol. 2(4):347-357, 1986.
7. Lindholm, U.S., Chan, K.S., Bodner, S.R., Weber, R.M., Walker, K.P., Cassenti, B.N., "Constitutive Modeling for Isotropic Materials (Host)," NASA-CR-174718, May 1984.
8. Beaman, R.L., "The Determination of the Bodner Material Coefficients for IN 718 and Their Effects on Cyclic Loading," Master's Thesis, AFIT/GAE/AA/84M-1, Air Force Institute of Technology, March, 1984.
9. Mercer, J.G., "Viscoplastic Analysis of Fatigue Cracks at Notches by the Finite-Element Method," Ph. D. Dissertation, AFIT/DS/AA/86D-2, Air Force Institute of Technology, December, 1986.
10. Hinnerichs, T.D., "Viscoplastic and Creep Crack Growth Analysis by the Finite Element Method," AFWAL-TR-80-4140, July 1981.
11. Stouffer, D.C., "A Constitutive Representation for IN 100," AFWAL-TR-4039, June 1981.
12. Perzyna, P., "Fundamental Problems in Viscoplasticity," *Advances in Applied Mechanics*, Vol. 9, 1966.
13. Cormeau, I., "Numerical Stability in Quasi-Static Elasto-Viscoplasticity," *International Journal for Numerical Methods in Engineering*, Vol. 9:109-127, 1975.
14. Ponter, A.R.S., *International Journal of Solids and Structures*, Vol. 16:793-806, 1980.
15. Hinnerichs, T.D., and Palazotto, A.N., "Viscoplasticity and Creep of a Three-Bar Linkage," *Journal of the Engineering Mechanics Division, Proceedings of the American Society of Civil Engineers*,

Technical Notes:567-571, June 1980.

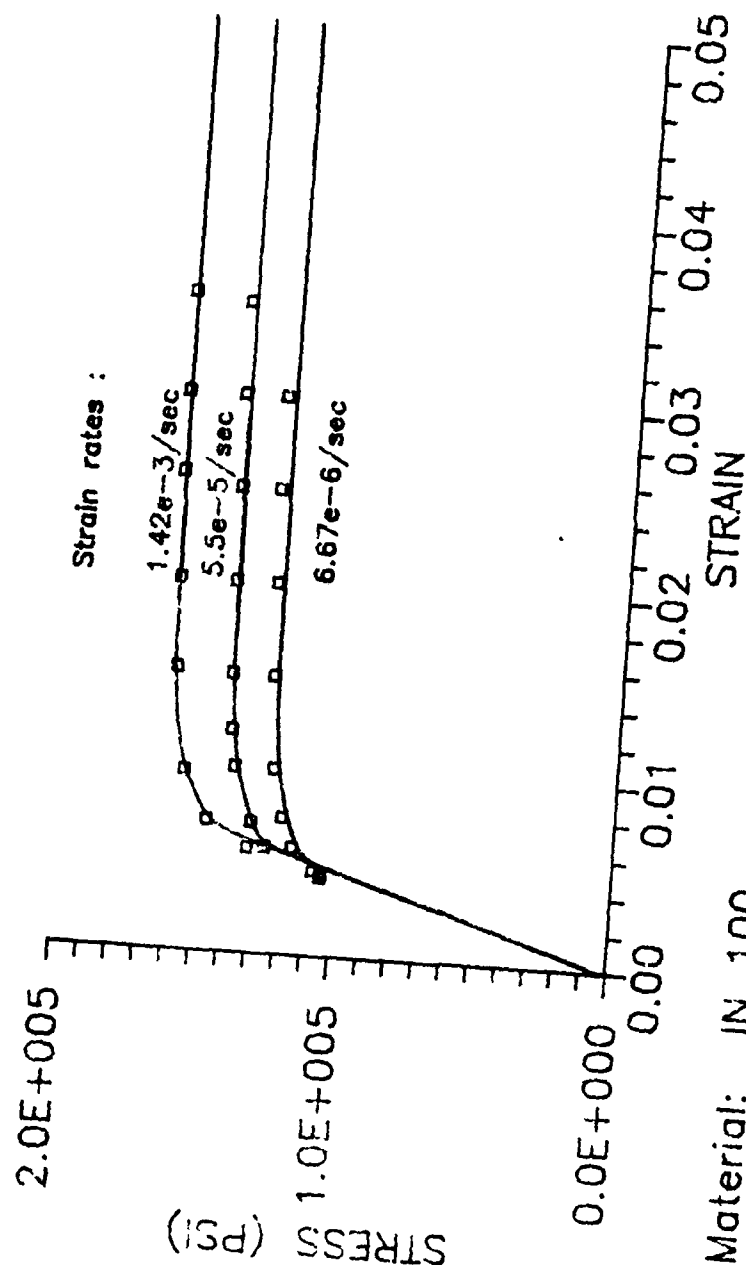
16. Kawahara, M., "Large Strain, Viscoelastic and Elasto-Viscoplastic Numerical Analysis using the Finite Element Method," Archives of Mechanics, Warsaw, Vol. 27(3), 1975.

## Appendix A

### Comparison of FINEL S Results with Stouffer's Predictions

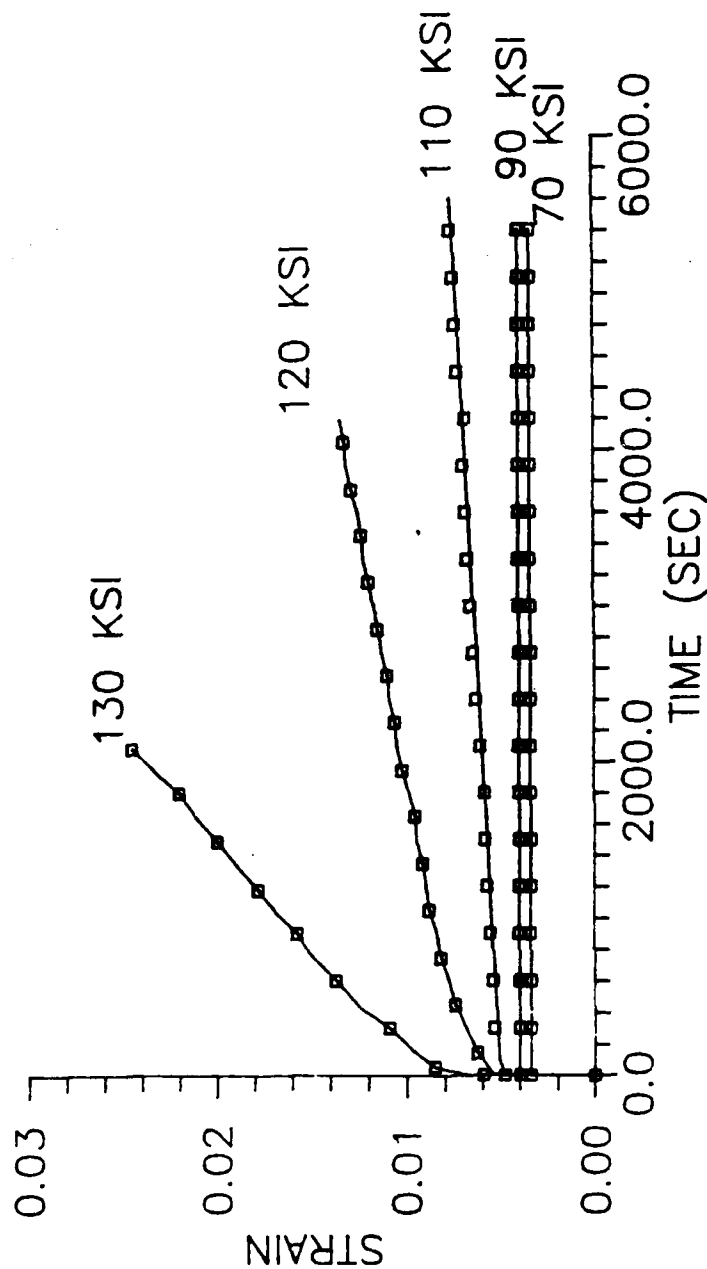
Stouffer (Ref 11) showed how to obtain Bodner-Partom constants for a material using data obtained from uniaxial tensile and creep tests. The constants thus obtained were then validated by comparing Bodner-Partom predictions with the test data used to obtain the constants. FINEL S was run using Stouffer's constants and the results compared to Stouffer's results and test data.

Stouffer calculated the Bodner-Partom constants for IN 100 to be those shown in Table I. The tensile test data was obtained from uniaxial tensile tests conducted using applied strain rates ranging from  $1.42 \times 10^{-3}/\text{sec}$  to  $1.67 \times 10^{-6}/\text{sec}$ . The creep test data was obtained from uniaxial tests conducted using applied stresses ranging from 72 KSI to 130 KSI. Stouffer predicted responses for applied stresses of 70 KSI, 90 KSI, 110 KSI, 120 KSI, and 130 KSI, and for applied strain rates of  $1.4 \times 10^{-3}/\text{sec}$ ,  $5.5 \times 10^{-5}/\text{sec}$ , and  $6.6 \times 10^{-6}/\text{sec}$ . The material behavior was predicted again using FINEL S with the same applied stresses and strain rates, and compared with Stouffer's predictions and test data as shown in Figures A-1 and A-2.



Symbols show Stouffer predictions.  
Lines show model predictions.

Figure A-1. Comparison of FINELS output with Stouffer's predictions.



Material: IN 100

Conditions: Uniaxial tension  
(Constant applied stress)

Symbols show Stouffer predictions.  
Lines show model predictions.

Figure A-2. Comparison of FINELS output with Stouffer's predictions.



## Appendix B

### The Three-Bar Linkage

The three-bar linkage, as originated by Kawahara (Ref 16) and expanded upon by Hinnerichs and Palazotto (Ref 15), is a method for simulating material behavior at a stress concentration by using uniaxial bar elements.

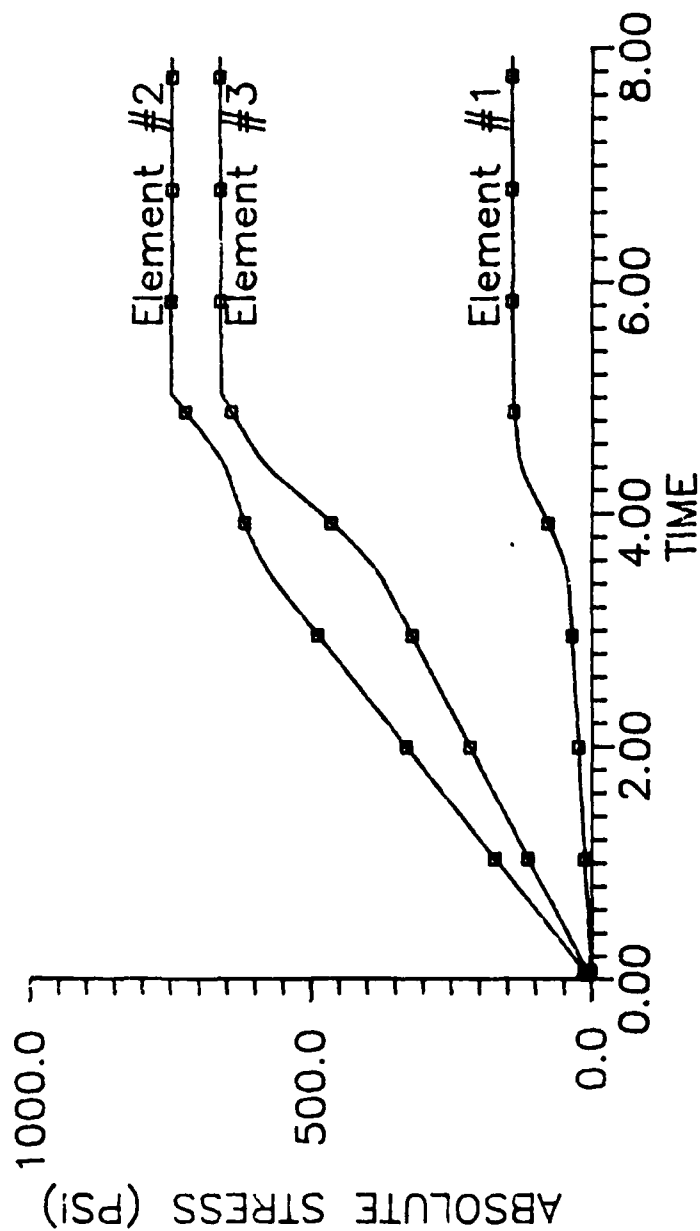
The three-bar linkage consists of three uniaxial bar elements as shown in Figure 21. Stress concentration is simulated by applying a load  $F$  at the central node, oriented such that the force acting upon one element is greater than those acting upon the other two. Viscoplasticity and creep can be included as described elsewhere in this paper.

FINELS was used to duplicate the results obtained by Hinnerichs and Palazotto (Ref 15) when they modelled the effects of viscoplasticity and creep in a three-bar linkage. The constants, time increments, and applied forces were calculated in the manner shown in Ref 15 and are shown in Table VII. The material's static stress-strain slope in the plastic region was modelled by assuming the yield stress to be linearly related to total strain, in this case

$$\begin{aligned}\sigma_Y &= [\sigma_Y]_0 + 0.1E(|\epsilon| - |\epsilon_Y|_0) & (|\epsilon| \geq |\epsilon_Y|_0) \\ &= [\sigma_Y]_0 & (|\epsilon| < |\epsilon_Y|_0)\end{aligned}$$

The first and second examples contained in Ref 15 were run using FINELS. The results are compared with those obtained by Hinnerichs and Palazotto in Figures B-1 and B-2. The third example was not attempted, as it deals with viscoelasticity which is not a primary concern of this effort.

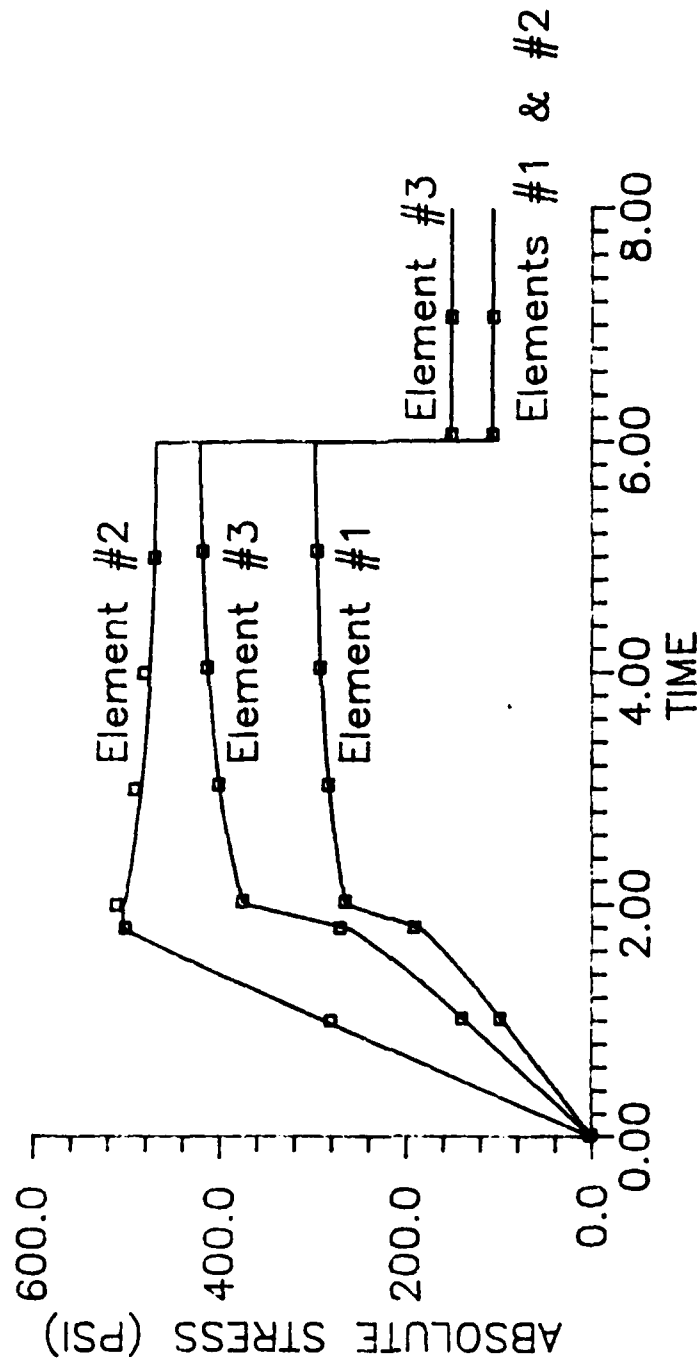
Table VII Three-Bar Linkage Conditions		
Parameter	Example #1	Example #2
$[\sigma_r]_0$	500 PSI	500 PSI
E	30,000 PSI	30,000 PSI
$\gamma$	166.667/sec	166.667/sec
n	1.0	1.0
$F_{\max}$	1250 lbs	765 lbs
$\gamma_c$	-	0.166667/sec
$\beta$	-	5.0
$\sigma_0$	-	1.0 PSI
dt	$3.33 \times 10^{-5}$ sec	$3.33 \times 10^{-5}$ sec



Peak force = 1250 lbs.

Symbols show Hinnerichs/Palazotto results for yield stress = 500 PSI.  
Lines show FINELS predictions.

Figure B-1. FINELS 3-bar Linkage Viscoplastic Response.



Peak force = 765 lbs.

Symbols show Hinnerichs/Palazotto results for yield stress = 500 PSI.  
Lines show FINELS predictions.

Figure B-2. FINELS 3-bar Linkage Viscoplastic and Creep Response.

## Appendix C

### Description of FEM Code

The program FINELS is a FEM code designed to predict viscoplasticity and creep in beam elements subjected to time-dependent stress or strains. FINELS can predict uniaxial behavior in single elements or can predict the behavior of structures containing several beam elements. Two versions exist, one of which uses Bodner-Partom constitutive law while the other uses combined Malvern Overstress theory and Norton's Law.

FINELS calculates elastic and viscoplastic stresses and strains using the residual force method in which, during a given time step  $i$ ,

$$[K]\{u\}^i = [F]^i + [Q]^{i-1} \quad (1)$$

where:

$[K]$  is the elastic stiffness matrix

$\{u\}$  is the nodal displacement matrix

$[F]$  is the matrix of applied forces

$[Q]$  is the matrix of residual forces

If the applied forces are specified, Equation 1 is solved for  $\{u\}$  by Gaussian elimination. If the nodal displacements are specified,  $[K]$  and  $\{u\}$  are multiplied to obtain  $[F]$ . Each term  $Q_i$  of the residual force matrix is calculated according to the plastic strains accumulated prior to the  $i$ th time step.

$$\begin{aligned} (Q_i)_x &= \sum_{n=1}^N E_n \epsilon_n^{inel} \cos \Theta_n \\ (Q_i)_y &= \sum_{n=1}^N E_n \epsilon_n^{inel} \sin \Theta_n \end{aligned} \quad (2)$$

where

$N$  = Total number of elements in system.

$n$  = Individual element identifier.

$\Theta_n$  = orientation angle of element  $n$ .

The nodal displacements, total strains, and stresses are then calculated for each member.

$$\{u\}^i = [K]^{-1} \left[ F \right]^i + [Q]^{i-1} \quad (3)$$

$$\{\epsilon\}^i = \left[ \frac{1}{L_n} \right] \{u\}^i \quad (4)$$

$$\{\sigma\}^i = [E] \left[ \{\epsilon\}^i - \{\epsilon^{inel}\}^{i-1} \right] \quad (5)$$

Viscoplastic and creep strain rates are then calculated and the total inelastic strain increased incrementally.

$$\{\dot{\epsilon}^P\}^i = f(\sigma, \epsilon^P) \quad (6)$$

$$\{\dot{\epsilon}^{VC}\}^i = g(\sigma) \quad (7)$$

$$\{\epsilon^{inel}\}^i = \{\epsilon^{inel}\}^{i-1} + \left[ \{\dot{\epsilon}^P\}^i + \{\dot{\epsilon}^{VC}\}^i \right] dt^i \quad (8)$$

Where the values of  $f$  and  $g$  are derived from the constitutive model or models used. Finally, the residual forces  $Q_i$  are recalculated for the new plastic strain values.

FINELS has five parts; a main program and four subroutines:

- The main program FINELS uses input data to construct global and constrained stiffness matrices.
- Subroutine SOLVE solves the matrix equation

$$[K] \{u\} = [F] + [Q]$$

for the nodal displacements  $\{u\}$  by Gaussian elimination.

- Subroutine TRN is the time integration routine used when the applied forces are specified. The applied force is assumed to be a sawtooth wave having specified maximum

- and minimum values and frequency. Subroutine SOLVE is used to compute nodal displacements due to the applied forces. Elastic and inelastic stresses and strains are then calculated as previously described for each time increment.
- Subroutine DISP is the time integration routine used when the nodal displacements are specified as functions of time. The nodal displacements are assumed to be sawtooth waves of known maximum and minimum value and frequency. Elastic and inelastic stresses and strains are then calculated for each time increment.
  - Subroutine READ reads data describing each element and node, including conditions of constraint.

#### DATA FILE CREATION:

FINELS reads list-directed input from a data file called "input", which must be set up as follows:

Line:	Data contained:	Variables:
1	OUTPUT1,OUTPUT2,OUTPUT3 (Output filenames)	OUTPUT1=output data file OUTPUT2=stress-strain plot file OUTPUT3=time plot file (See below)
2	NUMELS,NNODES	NUMELS=No. of elements NNODES=No. of nodes
Next N lines (N=NNODES)	$X_i, Y_i$	$X_i, Y_i$ =X and Y coordinates of node i.
Next M (M=NUMELS)	$I_{1j}, I_{2j}, A_j, E_j, I_1$	$I_1, I_2$ =Identification of first and second nodes, A=Cross-sectional area, E=Elastic modulus, I=Moment of inertia, of element j.

Next line	S or D	Specifies cyclic (S)ress or (D)isplacement (Strain)
-----------	--------	--

OVERSTRESS MODEL (Delete if Bodner model is used) :

BODNER MODEL (Delete if Overstress model is used) :

Next line	$D_0, Z_i, Z_0, Z_1, A, m, n, r$	Bodner-Partom material constants
-----------	----------------------------------	----------------------------------

Last line	FMAX,FMIN,UMAX,UMIN	Maximum and minimum values of applied force (FMAX,FMIN) and displacement (UMAX,UMIN).
-----------	---------------------	---

**FINELS** places output data in three files :

2. **OUTPUT2**. This file contains the data necessary to plot the stress-strain curve for one element, arranged in two columns. The first column contains



strains and the second stresses.

3. OUTPUT3. This file contains the data required to plot stress or strain vs. time. If strain control is selected, stresses will be plotted. If stress control is selected, strains will be plotted. The data is arranged in four columns, the first containing time and the rest containing stress or strain in elements 1, 2, and 3 respectively for each point in time.

Note that OUTPUT1, OUTPUT2, and OUTPUT3 are only the names of the internal variables which identify the external files. You can give these files whatever names you choose in line 1 of "input".

PROGRAM FINELS:

(See following pages)

```

*****
*
*      NOTE:
*
*      IF THE BODNER-PARTOM MODEL IS USED, USE FINELS AS SHOWN.  IF
*      OVERSTRESS/NORTON MODEL IS USED, SUBSTITUTE ALTERNATE VERSIONS
*      OF SUBROUTINES "TRN" AND "DISP" INSTEAD.
*
*****

```

```

      PROGRAM FINELS
      INTEGER NUMELS,NNODES,DOF,I1(10),I2(10),Z1,Z2,ZMAX,N,Z,P,I1,J,Q
      INTEGER Z1MAX,Z2MAX,R,CONSTR(40,3)
      REAL X1(10),Y1(10),X2(10),Y2(10),L(10),A(10),E(10),I(10)
      REAL THETA(10),KK(10,40,40),K(40,40),F(40),U(40),K1,K2
      CHARACTER*80 ANSWER
      OPEN(UNIT=9,FILE='testin',STATUS='OLD')

C
C      USE SUBROUTINE "READ" TO ENTER SYSTEM DATA.
C
      CALL READ(NUMELS,NNODES,I1,I2,A,E,I,X1,Y1,X2,Y2,CONSTR,F)

C
C      COMPUTE LOCAL STIFFNESS MATRICES FOR GENERALIZED BEAM ELEMENTS
C
      DOF=3
      DO 1001 N=1,NUMELS
      L(N)=SQRT(((X2(N)-X1(N))**2)+((Y2(N)-Y1(N))**2))
      THETA(N)=ASIN((Y2(N)-Y1(N))/L(N))
      Z1=(3*I1(N))-2
      Z2=(3*I2(N))-2
      Z1MAX=Z1+DOF-1
      Z2MAX=Z2+DOF-1
      DO 1 Z=Z1,Z1MAX
      DO 2 P=Z,Z2MAX
      IF(P.NE. Z1MAX .AND. Z.NE. Z1MAX)GO TO 3
      GO TO 4
3      IF(Z.EQ. Z1)GO TO 5
      GO TO 6
5      IF(P.EQ.Z)GO TO 7
      GO TO 8
7      K1=(A(N)*E(N))/L(N)
      K2=12.0*(E(N)*I(N))/(L(N)**3)
      KK(N,Z,P)=K1*(COS(THETA(N))**2)+K2*(SIN(THETA(N))**2)
8      IF(P.EQ.Z+1)GO TO 9
      GO TO 10
9      K1=(A(N)*E(N))/L(N)
      K2=12.0*(E(N)*I(N))/(L(N)**3)
      KK(N,Z,P)=(K1-K2)*SIN(THETA(N))*COS(THETA(N))
10     CONTINUE
6      IF(Z.EQ.Z1+1)GO TO 11
      GO TO 4
11     IF(P.EQ.Z)GO TO 13
      GO TO 14
13     K1=(A(N)*E(N))/L(N)
      K2=12.0*(E(N)*I(N))/(L(N)**3)
      KK(N,Z,P)=(K1*(SIN(THETA(N))**2)+K2*(COS(THETA(N))**2)

```

```

14          CONTINUE
4          IF(P.EQ.Z1MAX)GO TO 15
          GO TO 22
15          IF(Z.EQ.Z1)GO TO 17
          GO TO 18
17          KK(N,Z,P)=-6.0*((E(N)*I(N))/(L(N)**2))*(SIN(THETA(N)))
18          CONTINUE
          IF(Z.EQ.Z1+1)GO TO 19
          GO TO 20
19          KK(N,Z,P)=6.0*((E(N)*I(N))/(L(N)**2))*(COS(THETA(N)))
20          CONTINUE
          IF(Z.EQ.Z1MAX)GO TO 21
          GO TO 22
21          KK(N,Z,P)=4.0*(E(N)*I(N))/L(N)
22          CONTINUE
          KK(N,P,Z)=KK(N,Z,P)
2          CONTINUE
          DO 23 P=Z2,Z2MAX
          Q=P-Z2+Z1
          IF(P.LT.Z2MAX)KK(N,Z,P)=-KK(N,Z,Q)
          IF(P.EQ.Z2MAX.AND.Z.LT.Z1MAX)KK(N,Z,P)=KK(N,Z,Q)
          IF(P.EQ.Z2MAX.AND.Z.EQ.Z1MAX)KK(N,Z,P)=2.0*E(N)*I(N)/L(N)
          KK(N,P,Z)=KK(N,Z,P)
23          CONTINUE
1          CONTINUE
          DO 24 P=Z2,Z2MAX
          DO 25 Z=P,Z2MAX
          Q=P-Z2+Z1
          R=Z-Z2+Z1
          IF(P.LT.Z2MAX.AND.Z.LT.Z2MAX)KK(N,Z,P)=KK(N,R,Q)
          IF(P.EQ.Z2MAX.AND.Z.EQ.Z2MAX)KK(N,Z,P)=KK(N,R,Q)
          IF(P.EQ.Z2MAX.AND.Z.LT.Z2MAX)KK(N,Z,P)=-KK(N,R,P)
          IF(P.LT.Z2MAX.AND.Z.EQ.Z2MAX)KK(N,Z,P)=-KK(N,Z,Q)
          KK(N,P,Z)=KK(N,Z,P)
25          CONTINUE
24          CONTINUE
1001        CONTINUE
C
C          ADD LOCAL STIFFNESS MATRICES TO GET THE GLOBAL STIFFNESS MATRIX
C
          P=1
31          Z=1
29          N=1
27          K(P,Z)=K(P,Z)+KK(N,P,Z)
          N=N+1
          IF(N.GT.NUMELS)GO TO 26
          GO TO 27
26          Z=Z+1
          ZMAX=NNODES*DOF
          IF(Z.GT.ZMAX)GO TO 28
          GO TO 29
28          P=P+1
          IF(P.GT.ZMAX)GO TO 30
          GO TO 31
30          CONTINUE
          WRITE(7,*)'*****'
          WRITE(7,*)'GLOBAL STIFFNESS MATRIX [K]:'
          WRITE(7,*)'
          DO 3100 Q=1,ZMAX
          WRITE(7,*)(K(Q,J),J=1,ZMAX)

```

```

3100  CONTINUE
      WRITE(7,*)'*****'
C
C      INPUT APPLIED FORCES
C
      Z=1
33    Z=Z+1
      IF(Z.GT.ZMAX)GO TO 32
      GO TO 33
32    CONTINUE
      WRITE(7,*)'APPLIED FORCES [F]:'
      WRITE(7,*)'
      DO 3000 Q=1,ZMAX
          WRITE(7,*)F(Q)
3000  CONTINUE
C
C      APPLY DISPLACEMENT BOUNDARY CONDITIONS TO GLOBAL STIFFNESS MATRIX
C
      II=1
39    J=1
37    Z=(DOF*(II-1))+J
      IF(CONSTR(II,J).EQ.1)GO TO 34
      GO TO 35
34    J=J+1
      IF(J.GT.DOF)GO TO 36
      GO TO 37
36    II=II+1
      IF(II.GT.NNODES)GO TO 38
      GO TO 39
35    F(Z)=0.
      Z1=Z
      Z2=1
108   IF(Z2.EQ.Z1)GO TO 101
      GO TO 102
101    K(Z1,Z2)=1.
      GO TO 103
102    K(Z1,Z2)=0.
      K(Z2,Z1)=0.
103    Z2=Z2+1
      IF(Z2.GT.ZMAX)GO TO 34
      GO TO 108
38    CONTINUE
      WRITE(7,*)'*****'
      WRITE(7,*)'CONSTRAINED STIFFNESS MATRIX [K]:'
      WRITE(7,*)'
      DO 3200 Q=1,ZMAX
          WRITE(7,*)(K(Q,J),J=1,ZMAX)
3200  CONTINUE
      WRITE(7,*)'*****'
      WRITE(7,*)'TIME,ELEMENT,STRAIN,STRESS,DISPLACEMENT'
C
C      CALL THE VISCOPLASTICITY SUBROUTINES
C
      READ(9,*)ANSWER
      IF(ANSWER.EQ.'S')GO TO 901
      CALL DISP(NUMELS,ZMAX,X1,X2,Y1,Y2,I1,I2,L,U,E,A)
      GO TO 2001
901    CALL TRN(NUMELS,ZMAX,F,X1,X2,Y1,Y2,I1,I2,L,K,U,E,A)
2001  END
      SUBROUTINE SOLVE(ZMAX,K,F,U)

```

```

C
C
C
C
      DIAGONALIZE THE STIFFNESS MATRIX AND FORCE MATRIX
      BY GAUSSIAN ELIMINATION

      REAL K(40,40),F(40),U(40),K1,K2
      INTEGER M,N,P,Q,ZMAX
      P=1
304    K1=(K(P,P)**2)
      IF(SQRT(K1).GT.0.001)GO TO 300
      GO TO 2000
300    M=P+1
      F(P)=F(P)/K(P,P)
      IF(P.EQ.ZMAX)GO TO 305
      GO TO 306
305    K(P,P)=1.0
      GO TO 303
306    DO 5000 N=P+1,ZMAX
          K(P,N)=K(P,N)/K(P,P)
5000    CONTINUE
      K(P,P)=1.0
302    F(M)=F(M)-((K(M,P)/K(P,P))*F(P))
      K2=K(M,P)
      DO 5001 N=P,ZMAX
          K(M,N)=K(M,N)-((K2/K(P,P))*K(P,N))
5001    CONTINUE
      M=M+1
      IF(M.GT.ZMAX)GO TO 301
      GO TO 302
301    P=P+1
      IF(P.GT.ZMAX)GO TO 303
      GO TO 304
303    CONTINUE

C
C
C
      SOLVE THE SYSTEM OF EQUATIONS

      Q=ZMAX
403    M=1
401    F(M)=F(M)-((K(M,Q)/K(Q,Q))*F(Q))
      K(M,Q)=0.
      M=M+1
      IF(M.GE.Q)GO TO 400
      GO TO 401
400    Q=Q-1
      IF(Q.EQ.1)GO TO 402
      GO TO 403
402    CONTINUE

C
C
C
      PRINT THE DISPLACEMENTS

      Q=1
500    F(Q)=F(Q)/K(Q,Q)
      U(Q)=F(Q)
      Q=Q+1
      IF(Q.GT.ZMAX)GO TO 2001
      GO TO 500
2000    PRINT*, 'CHECK INPUTS'
2001    RETURN

      END

      SUBROUTINE TRN(NUMELS,ZMAX,F,X1,X2,Y1,Y2,I1,I2,L,K,U,E,A)
      REAL K(40,40),F(40),U(40),X1(20),X2(20),Y1(20),Y2(20)

```

```

REAL DT,T,TMAX,STRNBP(10),EDOT(10)
REAL FMAX,ANGLE,L1(10),STRN1(10),STRAIN(10),DISP(10),Q
REAL STRESS(10),E(10),A1,A2,L(10),KKK(40,40),YLDSTR(10)
REAL THETA(10),A(10),F1P(10),F2P(10),WP(10),ZZ(10),M,NN
INTEGER N,I1(10),I2(10),NUMELS,ZMAX,P1,P2,P,Z
DO 3 N=1,NUMELS
C
C   READ MINIMUM STRESS
C
C   READ(9,*)MINSTR(N)
C
C   CALCULATE ELEMENT ORIENTATION ANGLES
C
C   IF(X2(N).GE.X1(N))THETA(N)=ASIN((Y2(N)-Y1(N))/L(N))
C   IF(X2(N).LT.X1(N))THETA(N)=3.141593-ASIN((Y2(N)-Y1(N))/L(N))
C
C   INITIALIZE PARAMETERS
C
C   STRN1(N)=0.
C   STRAIN(N)=0.
C   STRESS(N)=0.
C   STRNBP(N)=0.
C   WP(N)=0.
C   EDOT(N)=0.
C   F1P(N)=0.
C   F2P(N)=0.
3   CONTINUE
C
C   READ MATERIAL PARAMETERS, TIME STEP AND LIMIT, FREQUENCY (HZ),
C   AND APPLIED MAX/MIN FORCES & NODAL DISPLACEMENTS
C
C   READ(9,*)DO,ZI,Z0,Z1,AA,M,NN,R
C   READ(9,*)DT,TMAX,FREQ
C   READ(9,*)FMAX,FMIN,UMAX,UMIN
C
C   DETERMINE THE NUMBER OF POINTS TO BE ENTERED AS DATA
C
C   QQQ=NUMELS*(INT(TMAX/(DT*500.0)))
C   IF(QQQ.LT.1)QQQ=1
C   WRITE(8,*)STRAIN(1),STRESS(1)
C   X=1.0
C   FF=0.
C   DO 4 T=0.,TMAX,DT
C
C   CALCULATE APPLIED FORCE MATRIX
C
C   IF(FF.GE.FMAX)X=-1.0
C   IF(FF.LE.FMIN)X=1.0
C   FF=FF+(2.*FREQ*(FMAX-FMIN)*X*DT)
C   ANGLE=0.
C   F(1)=(FF*COS(ANGLE))+F1P(1)+F1P(2)+F1P(3)
C   F(2)=(FF*SIN(ANGLE))+F2P(1)+F2P(2)+F2P(3)
C   DO 100 N=3,ZMAX
C   F(N)=0.
100  CONTINUE
C   DO 940 P=1,ZMAX
C   DO 941 Z=1,ZMAX
C   KKK(P,Z)=K(P,Z)
941  CONTINUE
940  CONTINUE

```

```

C
C
C      SOLVE FOR NODAL DISPLACEMENTS
C
C      CALL SOLVE(ZMAX, KKK, F, U)
2      CONTINUE
      DO 101 N=1, NUMELS
C
C      CALCULATE ELEMENTAL STRAINS AND STRESSES
C
      P1=(I1(N)*3)-2
      P2=(I2(N)*3)-2
      A1=(X2(N)-X1(N)+U(P2)-U(P1))*2
      A2=(Y2(N)-Y1(N)+U(P2+1)-U(P1+1))*2
      L1(N)=SQRT(A1+A2)
      STRN1(N)=(L1(N)/L(N))-1.0
      STRESS(N)=E(N)*(STRN1(N)-STRNBP(N))
      IF(STRESS(N).GE.0.)XXX=1.0
      IF(STRESS(N).LT.0.)XXX=-1.0
C
C      CALCULATE VISCOPLASTIC STRAINS
C
      ZZ(N)=Z1-(Z1-Z0)*EXP(-M*WP(N))
      IF(ABS(STRESS(N)).LT.YLDSTR(N))GO TO 501
      AAA=-(((ZZ(N)/STRESS(N))**2.0)**NN)*(NN+1.0)/NN
      D2P=(D0**2.0)*EXP(AAA)
      EDOT(N)=2.0*XXX*SQRT(D2P/3.0)
      GO TO 502
501      EDOT(N)=0.
502      STRNBP(N)=STRNBP(N)+(EDOT(N)*DT)
      ZREC=-AA*Z1*(((ZZ(N)-Z1)/Z1)**R)
      WP(N)=WP(N)+(STRESS(N)*EDOT(N)+(ZREC/(M*(Z1-ZZ(N)))))*DT
C
C      CALCULATE PLASTIC FORCES
C
      F1P(N)=-A(N)*E(N)*STRNBP(N)*COS(THETA(N))
      F2P(N)=-A(N)*E(N)*STRNBP(N)*SIN(THETA(N))
      STRAIN(N)=STRN1(N)
      DISP(N)=STRAIN(N)*L(N)
C
C      ENTER RESULTS INTO OUTPUT FILES
C
      Q=Q+1
      IF(Q.GE.QQQ)THEN
      Q=0
      WRITE(7,*)'*****'
      WRITE(7,*)T,'1',STRAIN(1),STRESS(1),DISP(1)
      WRITE(8,*)STRAIN(1),STRESS(1)
      WRITE(10,*)T,STRESS(1),STRESS(2),STRESS(3)
      ENDIF
101      CONTINUE
4      CONTINUE
      RETURN
      END
      SUBROUTINE DISP(NUMELS, ZMAX, X1, X2, Y1, Y2, I1, I2, L, U, E, A)
      REAL X1(10), X2(10), Y1(10), Y2(10), L(10), U(10), E(10), A(10)
      REAL STRAIN(10), STRNBP(10), T, TMAX, DT, L1(10), YLDSTR(10), M, NN
      REAL STRESS(10), K1, K2, ZZ(10), WP(10), EDOT(10)
      INTEGER N, I1(10), I2(10), ZMAX, P1, P2, NUMELS
      I=1
      DO 100 N=1, NUMELS

```

```

C
C READ MINIMUM STRESS
C
C READ(9,*)MINSTR(N)
C
C INITIALIZE PARAMETERS
C
C STRNBP(N)=0.
C STRAIN(N)=0.
C STRESS(N)=0.
C WP(N)=0.
100 CONTINUE
C
C READ MATERIAL PARAMETERS, TIME STEP AND LIMIT (SEC), FREQUENCY (HZ),
C AND APPLIED MAX/MIN FORCES & NODAL DISPLACEMENTS
C
C READ(9,*)D0,ZI,Z0,Z1,AA,M,NN,R
C READ(9,*)DT,TMAX,FREQ
C READ(9,*)FMAX,FMIN,UMAX,UMIN
C WRITE(8,*)STRAIN(1),STRESS(1)
C
C DETERMINE HOW MANY POINTS TO ENTER INTO OUTPUT DATA
C
C QQQ=NUMELS*(INT(TMAX/(DT*500.0)))
C IF(QQQ.LT.1)QQQ=1
C X=1.0
C UU=0.
C DO 1001 T=0.,TMAX,DT
C
C CALCULATE THE TIME-DEPENDENT DISPLACEMENT MATRIX
C
C IF(UU.GE.UMAX)X=-1.0
C IF(UU.LE.UMIN)X=1.0
C UU=UU+(2.*FREQ*(UMAX-UMIN)*X*DT)
C ANGLE=0.
C U(1)=UU*COS(ANGLE)
C U(2)=UU*SIN(ANGLE)
C DO 101 N=3,ZMAX
C U(N)=0.
101 CONTINUE
C DO 102 N=1,NUMELS
C
C CALCULATE STRAINS AND STRESSES
C
C P1=(I1(N)*3)-2
C P2=(I2(N)*3)-2
C K1=(X2(N)-X1(N)+U(P2)-U(P1))**2
C K2=(Y2(N)-Y1(N)+U(P2+1)-U(P1+1))**2
C L1(N)=SQRT(K1+K2)
C STRAIN(N)=(L1(N)/L(N))-1.0
C STRESS(N)=E(N)*(STRAIN(N)-STRNBP(N))
C IF(STRESS(N).GE.0.)YYY=1.0
C IF(STRESS(N).LT.0.)YYY=-1.0
C
C CALCULATE VISCOPLASTIC STRAINS
C
C ZZ(N)=Z1-(Z1-Z0)*EXP(-M*WP(N))
C IF(ABS(STRESS(N)).LT.YLDSTR(N))GO TO 501
C ZZZ=-(((ZZ(N)/STRESS(N))**2)**NN)*(NN+1.)/NN
C D2P=(D0**2)*EXP(ZZZ)

```



```

EDOT(N)=2.*YYY*SQRT(D2P/3.)
GO TO 502
501 EDOT(N)=0.
502 STRNBP(N)=STRNBP(N)+(EDOT(N)*DT)
ZREC=-AA*Z1*((ZZ(N)-ZI)/Z1)**R
XXX=ZREC/(M*(Z1-ZZ(N)))
WP(N)=WP(N)+((STRESS(N)*EDOT(N))+XXX)*DT)

C
C ENTER RESULTS INTO OUTPUT FILES
C
Q=Q+1
IF(Q.GE.QQQ)THEN
Q=0
WRITE(7,*)'*****'
WRITE(7,*)T,N,STRAIN(N),STRESS(N),U(1)
IF(N.EQ.1)WRITE(8,*)STRAIN(1),STRESS(1)
IF(N.EQ.1)WRITE(10,*)T,STRESS(1),STRESS(2),STRESS(3)
ENDIF
102 CONTINUE
1001 CONTINUE
RETURN
END
SUBROUTINE READ(NUMELS,NNODES,I1,I2,A,E,I,X1,Y1,X2,Y2,CONSTR,F)
REAL A(10),E(10),I(10),X1(10),X2(10),X(40),Y1(10),Y2(10),Y(40)
REAL F(40)
INTEGER NUMELS,NNODES,I1(10),I2(10),CONSTR(40,3),II,J,Z
CHARACTER*20 OUTPUT1,OUTPUT2,OUTPUT3
READ(9,*)OUTPUT1,OUTPUT2,OUTPUT3
OPEN(UNIT=7,FILE=OUTPUT1,STATUS='NEW')
OPEN(UNIT=8,FILE=OUTPUT2,STATUS='NEW')
OPEN(UNIT=10,FILE=OUTPUT3,STATUS='NEW')

C
C READ NUMBER OF ELEMENTS AND NODES
C
READ(9,*)NUMELS,NNODES

C
C READ NODE LOCATIONS
C
DO 1 II=1,NNODES
READ(9,*)X(II),Y(II)
1 CONTINUE

C
C READ DATA NECESSARY TO DESCRIBE EACH ELEMENT (NODES AND PROPERTIES)
C
DO 100 N=1,NUMELS
READ(9,*)I1(N),I2(N),A(N),E(N),I(N)
X1(N)=X(I1(N))
Y1(N)=Y(I1(N))
X2(N)=X(I2(N))
Y2(N)=Y(I2(N))
100 CONTINUE

C
C CONDITIONS OF CONSTRAINT (1 = FREE, 0 = CONSTRAINED)
C
DO 101 II=1,NNODES
READ(9,*)(CONSTR(II,J),J=1,3)
101 CONTINUE

C
C READ F(X),F(Y),AND M(XY) AT EACH NODE
C

```

DO 102 II=1,NNODES  
Z=(3\*II)-2  
102 READ(9,\*)F(Z),F(Z+1),F(Z+2)  
CONTINUE  
RETURN  
END

```

*****
*
*   NOTE:
*
*   IF THE OVERSTRESS/NORTON MODEL IS TO BE USED, USE THESE
*   VERSIONS OF SUBROUTINES "TRN" AND "DISP" IN PLACE OF THE
*   BODNER-PARTOM VERSIONS.
*
*****

```

```

SUBROUTINE TRN(NUMELS,ZMAX,F,X1,X2,Y1,Y2,I1,I2,L,K,U,E,A)
REAL K(40,40),F(40),U(40),X1(20),X2(20),Y1(20),Y2(20)
REAL STRNP(10),DT,T,TMAX,YLDSTR(10),GAMMA(10),NEXP(10)
REAL FMAX,ANGLE,L1(10),STRN1(10),STRAIN(10),DISP(10),Q
REAL STRESS(10),EPDOT(10),E(10),A1,A2,L(10),KKK(40,40)
REAL THETA(10),A(10),F1P(10),F2P(10),STRNVC(10),WP(10)
REAL GAMC(10),BETA(10)
INTEGER N,I1(10),I2(10),NUMELS,ZMAX,P1,P2,P,Z
DO 3 N=1,NUMELS

C
C   READ YIELD STRESS, VISCOPLASTIC CONSTANTS, AND CREEP CONSTANTS
C
C   READ(9,*)YLDSTR(N),GAMMA(N),NEXP(N),GAMC(N),BETA(N)

C
C   CALCULATE ELEMENT ORIENTATION ANGLES
C
C   IF(X2(N).GE.X1(N))THETA(N)=ASIN((Y2(N)-Y1(N))/L(N))
C   IF(X2(N).LT.X1(N))THETA(N)=3.141593-ASIN((Y2(N)-Y1(N))/L(N))

C
C   INITIALIZE PARAMETERS
C
C   Q=0
C   STRN1(N)=0.
C   STRAIN(N)=0.
C   STRNP(N)=0.
C   STRNVC(N)=0.
C   STRESS(N)=0.
C   F1P(N)=0.
C   F2P(N)=0.
3  CONTINUE

C
C   READ IN TIME STEP AND LIMIT (SEC), FREQUENCY (HZ), AND APPLIED
C   MAX/MIN FORCES & NODAL DISPLACEMENTS
C
C   READ(9,*)DT,TMAX,FREQ
C   READ(9,*)FMAX,FMIN,UMAX,UMIN
C   WRITE(8,*)STRAIN(1),STRESS(1)
C   QQQ=NUMELS*(INT(TMAX/(DT*500.0)))
C   IF(QQQ.LT.1)QQQ=1
C   X=1.0
C   FF=0.
C   DO 1000 T=0.,TMAX,DT

C
C   CALCULATE TIME-DEPENDENT APPLIED FORCE MATRIX
C

```

```

IF(FF.GE.FMAX)X=-1.0
IF(FF.LE.FMIN)X=1.0
FF=FF+(2.*X*FREQ*(FMAX-FMIN)*DT)
ANGLE=0.
F(1)=(FF*COS(ANGLE))+F1P(1)+F1P(2)+F1P(3)
F(2)=(FF*SIN(ANGLE))+F2P(1)+F2P(2)+F2P(3)
      DO 100 N=3,ZMAX
      F(N)=0.
100      CONTINUE
      DO 940 P=1,ZMAX
      DO 941 Z=1,ZMAX
      KKK(P,Z)=K(P,Z)
941      CONTINUE
940      CONTINUE
C
C      SOLVE FOR NODAL DISPLACEMENTS
C
      CALL SOLVE(ZMAX,KKK,F,U)
      DO 101 N=1,NUMELS
      AAA=0.002*WP(N)
C
C      CALCULATE STRAIN-DEPENDENT YIELD STRESS
C
      YLDSTR(N)=100000.*(0.9+(0.2*EXP(-AAA)))
C
C      CALCULATE ELEMENTAL STRAINS AND STRESSES
C
      P1=(I1(N)*3)-2
      P2=(I2(N)*3)-2
      A1=(X2(N)-X1(N)+U(P2)-U(P1))*2
      A2=(Y2(N)-Y1(N)+U(P2+1)-U(P1+1))*2
      L1(N)=SQRT(A1+A2)
      STRN1(N)=(L1(N)/L(N))-1.0
      STRESS(N)=E(N)*(STRN1(N)-STRNP(N)-STRNVC(N))
      IF(ABS(STRESS(N)).LT.10.0)GO TO 50
      GO TO 21
50      ZZZ=0.
      GO TO 22
C
C      CALCULATE CREEP STRAIN RATE
C
21      ZZZ=ABS(STRESS(N))/STRESS(N)
22      ZZQ=DT*GAMC(N)*ZZZ*((ABS(STRESS(N))*BETA(N))
      IF(ABS(STRESS(N)).GE.YLDSTR(N))ZZQ=0.
      STRNVC(N)=ZZQ+STRNVC(N)
C
C      CALCULATE VISCOPLASTIC STRAIN RATE
C
      IF(ABS(STRESS(N)).GE.YLDSTR(N))GO TO 10
      GO TO 20
10      ZZZ=ZZZ*GAMMA(N)
      EPDOT(N)=ZZP*((ABS(STRESS(N))/YLDSTR(N))-1.)*NEXP(N))
      WP(N)=WP(N)+(STRESS(N)*EPDOT(N)*DT)
      STRNP(N)=(EPDOT(N)*DT)+STRNP(N)
C
C      CALCULATE NEW PLASTIC FORCES
C
20      F1P(N)=-A(N)*E(N)*(STRNP(N)+STRNVC(N))*COS(THETA(N))
      F2P(N)=-A(N)*E(N)*(STRNP(N)+STRNVC(N))*SIN(THETA(N))
      STRAIN(N)=STRN1(N)

```

```

      DISP(N)=STRAIN(N)*L(N)
C
C
C      ENTER RESULTS INTO OUTPUT FILES
      Q=Q+1
      IF(Q.GE.QQQ)THEN
      Q=0
      WRITE(7,*)'*****'
      WRITE(7,*)T,N,STRAIN(N),STRESS(N),DISP(N)
      WRITE(7,*)EPDOT,ZZQ,STRNP(N),STRNVC(N),YLDSTR(N),F1P(N),F2P(N)
      WRITE(8,*)STRAIN(1),STRESS(1)
      WRITE(10,*)T,STRAIN(1),STRAIN(2),STRAIN(3)
      ENDIF
101    CONTINUE
1000   CONTINUE
      RETURN
      END
      SUBROUTINE DISP(NUMELS,ZMAX,X1,X2,Y1,Y2,I1,I2,L,U,E,A)
      REAL X1(10),X2(10),Y1(10),Y2(10),L(10),U(10),E(10),A(10)
      REAL STRAIN(10),STRNP(10),T,TMAX,DT,L1(10),YLDSTR(10)
      REAL GAMMA(10),NEXP(10),EPDOT,STRESS(10),K1,K2,STRNVC(10)
      REAL WP(10),GAMC(10),BETA(10)
      INTEGER N,I1(10),I2(10),ZMAX,P1,P2,NUMELS
      I=1
      DO 100 N=1,NUMELS
C
C
C      READ YIELD STRESS, VISCOPLASTIC CONSTANTS, AND CREEP CONSTANTS
      READ(9,*)YLDSTR(N),GAMMA(N),NEXP(N),GAMC(N),BETA(N)
C
C
C      CALCULATE ELEMENT ORIENTATION ANGLES
      STRNP(N)=0.
      STRNVC(N)=0.
      STRAIN(N)=0.
      STRESS(N)=0.
100    CONTINUE
C
C
C      READ IN TIME STEP AND LIMIT (SEC), FREQUENCY (HZ), AND APPLIED
      MAX/MIN FORCES & NODAL DISPLACEMENTS
      READ(9,*)DT,TMAX,FREQ
      READ(9,*)FMAX,FMIN,UMAX,UMIN
      WRITE(8,*)STRAIN(1),STRESS(1)
      QQQ=NUMELS*(INT(TMAX/(DT*500.0)))
      IF(QQQ.LT.1)QQQ=1
      X=1.0
      UU=0.
      DO 1001 T=0.,TMAX,DT
C
C
C      CALCULATE TIME-DEPENDENT DISPLACEMENT MATRIX
      IF(UU.GE.UMAX)X=-1.0
      IF(UU.LE.UMIN)X=1.0
      UU=UU+(2.*X*FREQ*(UMAX-UMIN)*DT)
      ANGLE=0.
      U(1)=UU*COS(ANGLE)
      U(2)=UU*SIN(ANGLE)
      DO 101 N=3,ZMAX
      U(N)=0.

```

```

101    CONTINUE
      DO 102 N=1,NUMELS
C
C      CALCULATE ELEMENTAL STRAINS AND STRESSES
C
        P1=(I1(N)*3)-2
        P2=(I2(N)*3)-2
        K1=(X2(N)-X1(N)+U(P2)-U(P1))*2
        K2=(Y2(N)-Y1(N)+U(P2+1)-U(P1+1))*2
        L1(N)=SQRT(K1+K2)
        STRAIN(N)=(L1(N)/L(N))-1.0
        STRESS(N)=E(N)*(STRAIN(N)-STRNP(N)-STRNVC(N))
C
C      CALCULATE CREEP STRAIN RATE
C
        ZZZ=ABS(STRESS(N))/STRESS(N)
        ZZQ=DT*GAMC(N)*ZZZ*((ABS(STRESS(N))*BETA(N))
        IF(ABS(STRESS(N)).GE.YLDSTR(N))ZZQ=0.
        STRNVC(N)=ZZQ+STRNVC(N)
C
C      CALCULATE STRAIN-DEPENDENT YIELD STRESS
C
        AAA=0.002*WP(N)
        YLDSTR(N)=100000.*(0.9+(.2*EXP(-AAA)))
        IF(ABS(STRESS(N)).GE.YLDSTR(N))GO TO 200
        GO TO 300
C
C      CALCULATE VISCOPLASTIC STRAIN RATE
C
200    ZZP=ZZZ*GAMMA(N)
        EPDOT=ZZP*((ABS(STRESS(N))/YLDSTR(N))-1.)*NEXP(N)
        WP(N)=WP(N)+(STRESS(N)*EPDOT*DT)
        STRNP(N)=STRNP(N)+(EPDOT*DT)
300    CONTINUE
C
C      ENTER RESULTS INTO OUTPUT FILES
C
        Q=Q+1
        IF(Q.GE.QQQ)THEN
          Q=0
          WRITE(7,*)'*****'
          WRITE(7,*)T,N,STRAIN(N),STRESS(N),U(1)
          IF(N.EQ.1)WRITE(8,*)STRAIN(1),STRESS(1)
          IF(N.EQ.1)WRITE(10,*)T,STRESS(1),STRESS(2),STRESS(3)
          ENDIF
102    CONTINUE
1001  CONTINUE
      RETURN
      END

```

INPUT FILE "TESTIN" (BODNER-PARTOM MODEL)

dat100,ss100,time100

3,4

0,0

-1,1

-1,-1

1.4142,0

1,2,1.0,26.3E6,0

1,3,1.0,26.3E6,0

1,4,1.0,26.3E6,0

1,1,0

0,0,0

0,0,0

0,0,0

0,0,0

0,0,0

0,0,0

0,0,0

S

100

100

100

1.E4,600000,915000,1015000,1.9E-3,2.57E-3,0.7,2.66

0.01,6,4.166667E-2

300000,-300000,.008,-.008

INPUT FILE "TESTIN" (OVERSTRESS/NORTON MODEL)

dat413,ss413,time413

3,4

0,0

-1,1

-1,-1

1.4142,0

1,2,1.0,25.05E6,0

1,3,1.0,25.05E6,0

1,4,1.0,25.05E6,0

1,1,0

0,0,0

0,0,0

0,0,0

0,0,0

0,0,0

0,0,0

0,0,0

0,0,0

S

130000,.0107,1,1,520E-26,4.022

130000,.0107,1,1,520E-26,4.022

130000,.0107,1,1,520E-26,4.022

0.1,600,1.666667E-3

200000.,-200000.,.008,-.008



## Vita

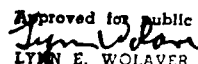
David Allen Shaffer was born on 6 March 1961 in Clearfield, Pennsylvania. He graduated from Clearfield High School in 1979 and attended the Pennsylvania State University from which he received the degree of Bachelor of Aerospace Engineering in August 1983. Upon graduation, he received a commission in the USAF through the ROTC program. He was assigned to Wright-Patterson AFB in November 1983 and has since served under the Aeronautical Systems Division Deputy for Engineering and the B-1 System Program Office as a Fuel Systems Development Engineer. He entered the School of Engineering, Air Force Institute of Technology, as a part-time student in October 1984.

UNCLASSIFIED

SECURITY CLASSIFICATION OF THIS PAGE

## REPORT DOCUMENTATION PAGE

Form Approved  
OMB No. 0704-0188

1a. REPORT SECURITY CLASSIFICATION Unclassified			1b. RESTRICTIVE MARKINGS		
2a. SECURITY CLASSIFICATION AUTHORITY			3. DISTRIBUTION / AVAILABILITY OF REPORT Approved for public release; distribution unlimited		
2b. DECLASSIFICATION / DOWNGRADING SCHEDULE			5. MONITORING ORGANIZATION REPORT NUMBER(S)		
4. PERFORMING ORGANIZATION REPORT NUMBER(S) AFIT/ GAE/ AA/ 87D-21			7a. NAME OF MONITORING ORGANIZATION		
6a. NAME OF PERFORMING ORGANIZATION Air Force Institute of Technology		6b. OFFICE SYMBOL (If applicable) ENY	7b. ADDRESS (City, State, and ZIP Code)		
6c. ADDRESS (City, State, and ZIP Code) Wright-Patterson AFB, OH 45433-8503			9. PROCUREMENT INSTRUMENT IDENTIFICATION NUMBER		
8a. NAME OF FUNDING / SPONSORING ORGANIZATION Air Force Wright Aeronautical Laboratories		8b. OFFICE SYMBOL (If applicable) AFWAL/MLLN	10. SOURCE OF FUNDING NUMBERS		
8c. ADDRESS (City, State, and ZIP Code) Wright-Patterson AFB, OH 45433-8503			PROGRAM ELEMENT NO. 61102F	PROJECT NO. 2302	TASK NO. P1
			WORK UNIT ACCESSION NO. 01		
11. TITLE (Include Security Classification) An Investigation of Constitutive Models for Predicting Viscoplastic Response During Cyclic Loading (Unclassified)					
12. PERSONAL AUTHOR(S) David A. Shaffer, Capt USAF					
13a. TYPE OF REPORT MS Thesis		13b. TIME COVERED FROM _____ TO _____		14. DATE OF REPORT (Year, Month, Day) June 1988	
15. PAGE COUNT 85					
16. SUPPLEMENTARY NOTATION					
<p style="text-align: right;">Approved for public release: 1AW AFR 190-11            LYNN E. WOLAVER          Dean for Research and Professional Development          Wright-Patterson AFB, OH 45433</p>					
17. COSATI CODES			18. SUBJECT TERMS (Continue on reverse if necessary and identify by block number)		
FIELD	GROUP	SUB-GROUP	Bodner-Partom Constitutive Law		
20	11		Creep		
			Viscoplasticity		
19. ABSTRACT (Continue on reverse if necessary and identify by block number)					
<p>An investigation of the Bodner-Partom model for determining viscoplastic deformation of high-temperature turbine engine alloys was conducted to determine its ability to predict cyclic behavior. A one-dimensional finite element method (FEM) code was developed using the Bodner-Partom constitutive model to predict the frequency-dependent yielding of uniaxial tensile specimens of nickel-based superalloys subjected to cyclic loads and strains comprising a range of frequencies and amplitudes. The predictions are compared to test data and discrepancies noted. The Bodner-Partom predictions are also compared to predictions developed using Overstress theory and Norton's Law for Secondary Creep in a similar FEM code. A three-bar linkage model is then developed to illustrate viscoplastic behavior at a stress concentration. Areas requiring further study are identified.</p>					
20. DISTRIBUTION / AVAILABILITY OF ABSTRACT UNCLASSIFIED/UNLIMITED <input checked="" type="checkbox"/> SAME AS RPT. <input type="checkbox"/> DTIC USERS			21. ABSTRACT SECURITY CLASSIFICATION Unclassified		
22a. NAME OF RESPONSIBLE INDIVIDUAL David A. Shaffer, Capt USAF			22b. TELEPHONE (Include Area Code) (513) 255-5440		22c. OFFICE SYMBOL ASD/BIEFP

DD Form 1473, JUN 86

Previous editions are obsolete.

SECURITY CLASSIFICATION OF THIS PAGE

UNCLASSIFIED